School on X-ray Imaging Techniques at the ESRF

February 5-6, 2007

Medical imaging, radiobiology and radiotherapy

Alberto Bravin

ID17 Bio-Medical Beamline

bravin@esrf.fr

Outline

- Introduction
- SR Imaging techniques (K-edge, Temporal subtraction imaging, Analyser based imaging)
- Selected applications: mammography, bone and cartilage, brain imaging
- Radiotherapy and radiobiology
- Radiotherapy with SR
- Applications: Microbeam Radiation Therapy (MRT), Stereotactic Synchrotron Radiation Therapy (SSRT)

SR (Bio) Medical Programs

1 ESRF (Grenoble, France)
2 ELETTRA (Trieste, Italy)
3 DESY (Hamburg, Germany)
4 SRS (Daresbury, UK)
5 BNL (Upton, USA)
6 APS (Chicago, USA)
7 SPRING8 (Himeji, Japan)

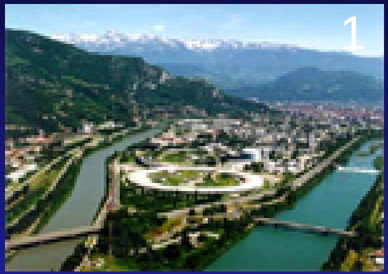

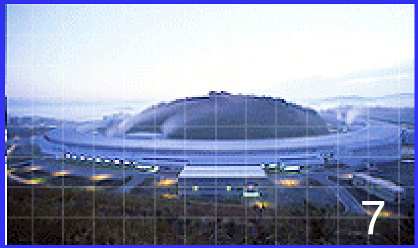

Dedicated facilities for
Medical Applications: 1,2,7

Coming soon: Melbourne and Saskatoon (dedicated)

ID17 Biomedical beamline Layout

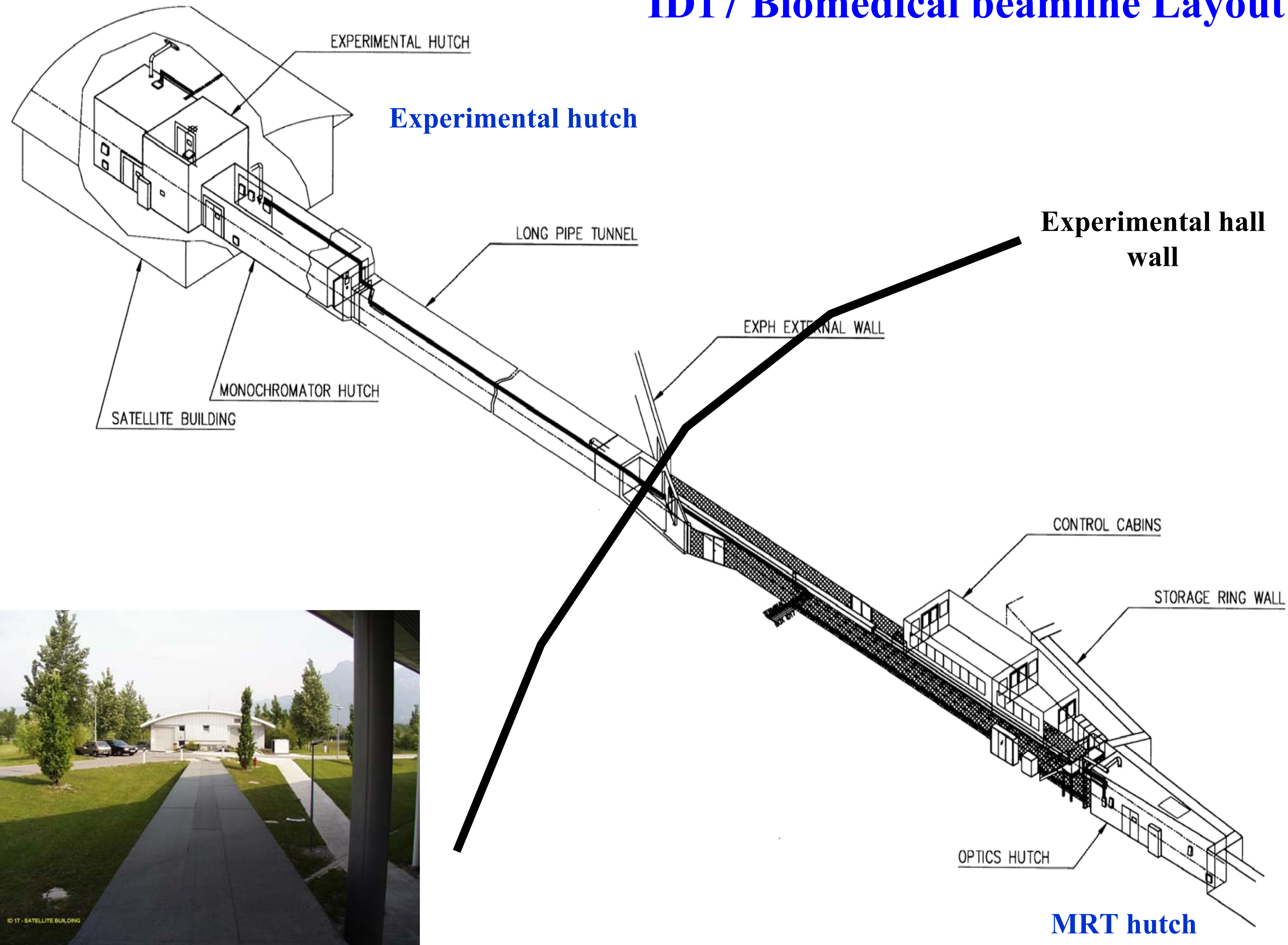

Bio-Medical beamline (ID17)

Mission: **Clinically-oriented** research:

- Medical imaging
- Radiobiology
- Radiation Therapy

Clinically (=patients) oriented:

• Preclinical research contributing to the clinical medicine in hospitals (testing new drugs, contrast agents, finding origin of illness, measure physiological parameters, study the effect of radiation on cells/tissues etc)
• Perform clinical research when it is only possible with SR (angiography, radiotherapy)

Preclinical research is done in phantoms, cells, animal models

Imaging

Why SR light for medical imaging?

Intense, collimated and polarized source of X-rays in a wide energy range (1- 100 keV)

- Monochromaticity (no beam hardening, quantitative projection and CT, K-edge imaging, energy optimisation with sample, dose reduction…)
- Collimation (highly reduced scattering on the images), parallel beam (no cone beam effects)
- Collimation+ small source (coherence): phase contrast imaging
- (Linearly) Polarized (reduced scattering)
- Flexible setup: combination of different techniques (CT + fluorescence + EXAFS….)

Biomedical Imaging Methods @ ESRF

	Applications	In vivo?	Lectures
Absorption	Bone	Y	P. Bluet, M. Salome
K-edge imaging (energy or temporal subtraction)	Angiography, Bronchography, Vascular, Brain perfusion	Y	This lecture
PhC: propagation	µvascularization, Bone, Mammography	Y	P. Cloetens
PhC: Analyser based imaging	Bone, Mammography, Lungs	Y	This lecture
CT+fluorescence	µquantification, Cells	Y/N	S. Bohic

Key words in SR biomedical imaging

- Large field of view (20 cm?)-skulls/chest
- High resolution (< 50 micron, down to 1 micron)
- In vivo
- Dose limited
- Fast imaging (functional, K-Edge imaging)
- Combination of techniques in situ
- Fast (on-line?) analysis of results

Interaction of X-rays with tissues (pictorial)

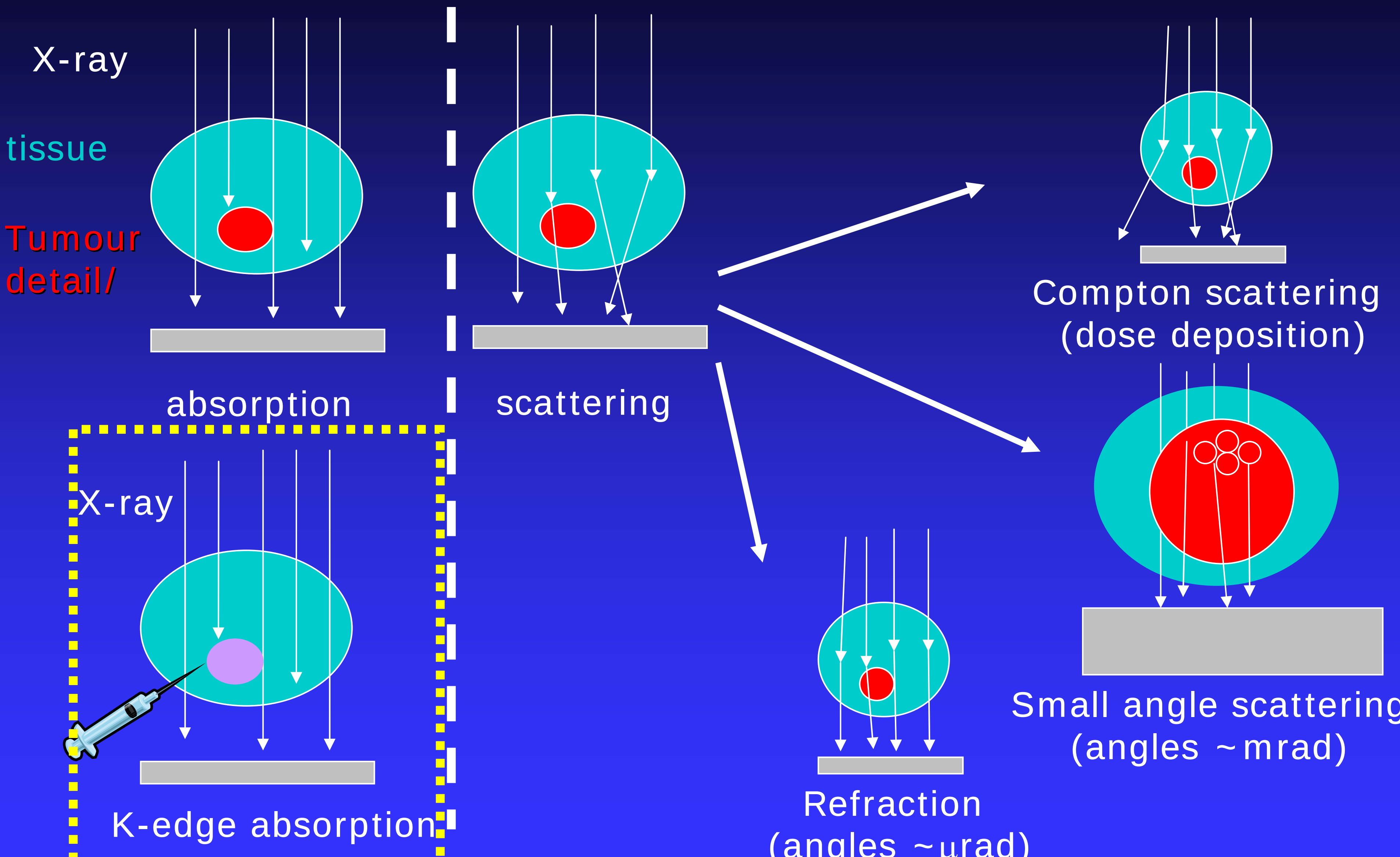

http://detserv1.dl.ac.uk/Herald/xray_history.htm

The
Energy (K)-edge subtraction imaging technique

Iodine absorption coefficient

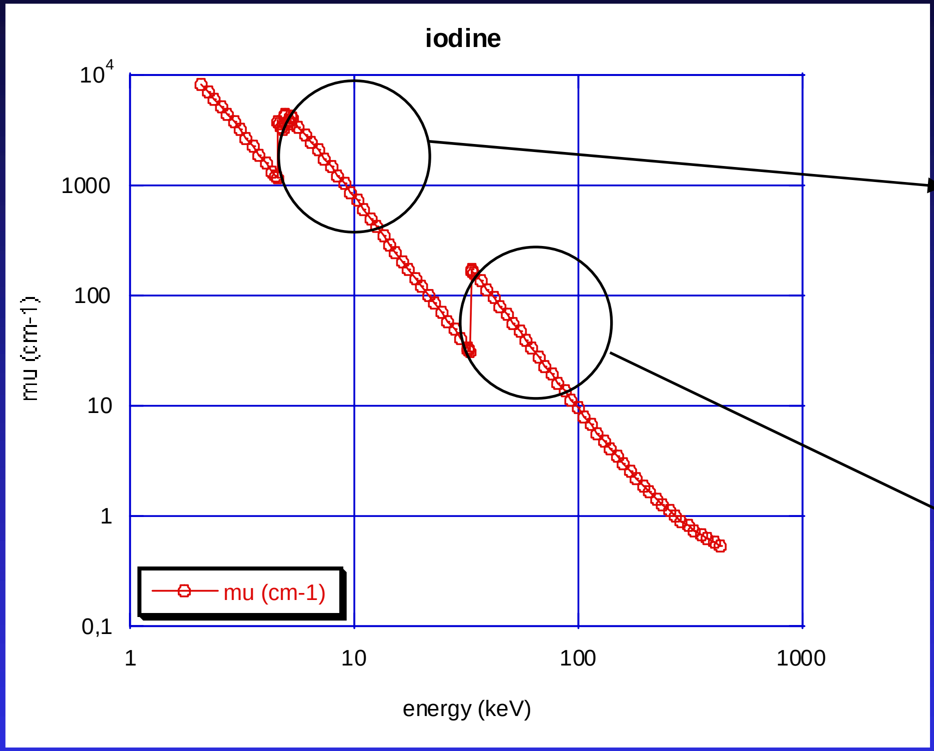

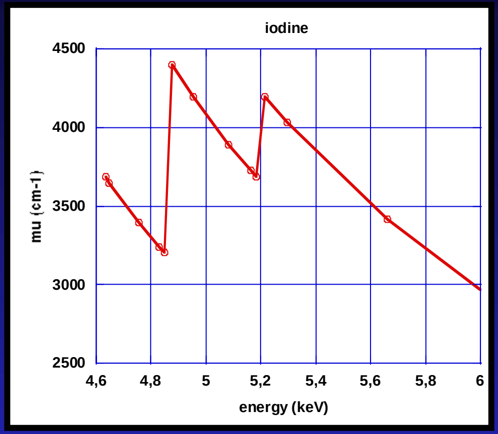

L-edges

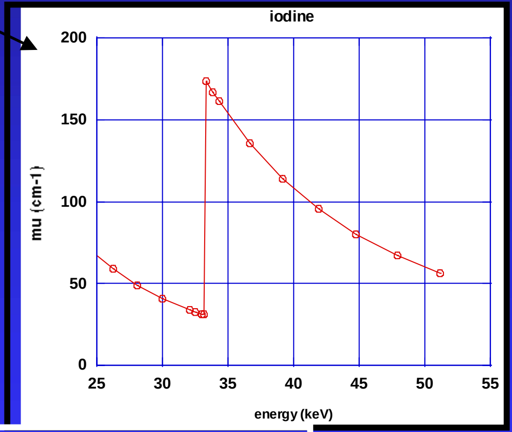

K-edge

Edge energies (keV)

K 3.31694E+01	L I 5.18810E+00	M I 1.07210E+00
	L II 4.85210E+00	M II 9.30500E-01
	L III 4.55710E+00	M III 8.74600E-01
		M IV 6.31300E-01
		M V 6.19400E-01

K-edge Subtraction

1. Contrast agent injection: Iodine, Gadolinium, Xenon etc.
2. Two Images: Above (A) and Below (B) the K-edge
3. Image processing : “Contrast agent” and Tissue images

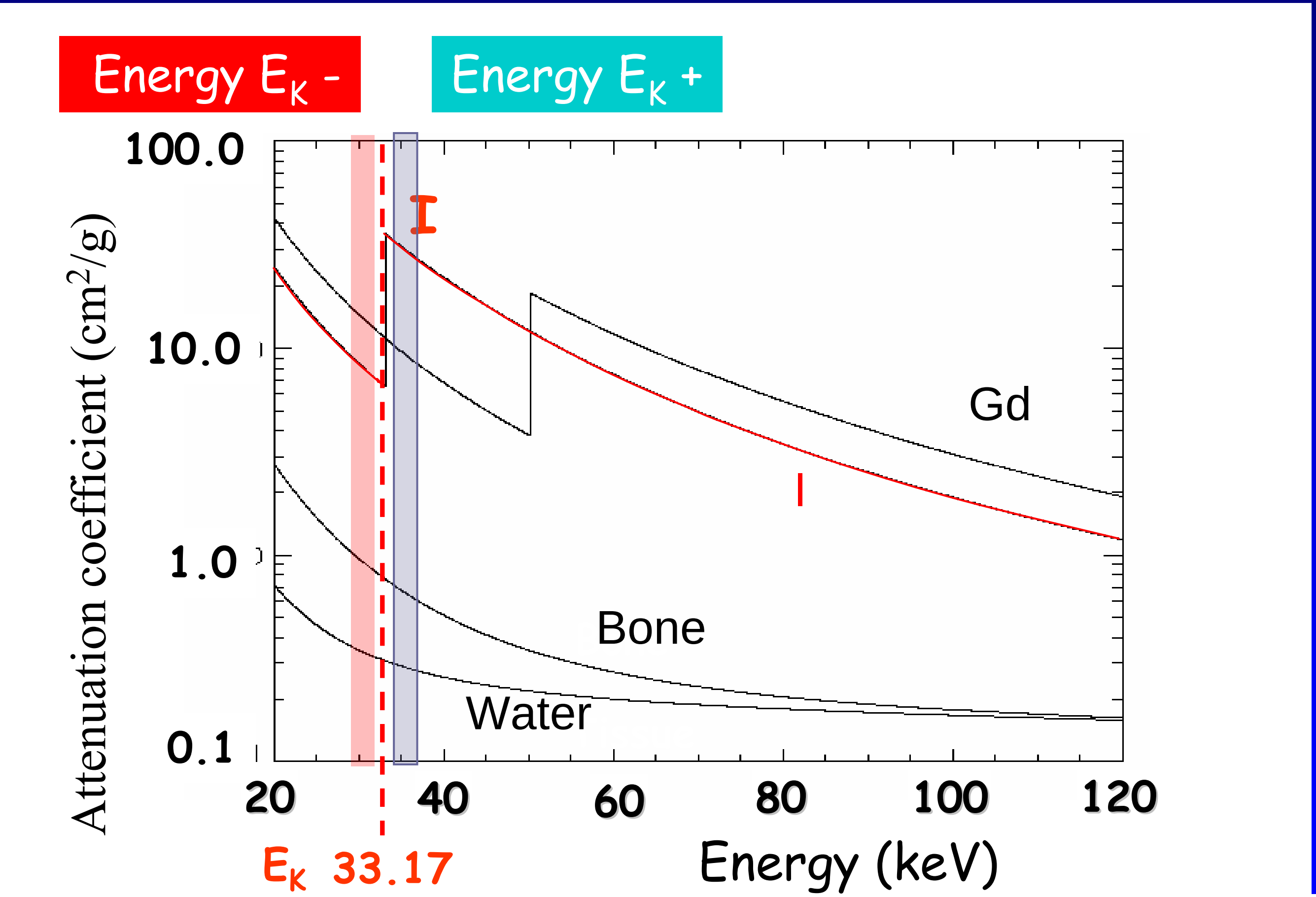

Signal

- Number of detected photons per pixel N in the image with energy E and is related to the number of incident photons N_0 by (Beer-Lambert law):

$$N = N_0 \exp\left[-\sum_j \left(\frac{\mu}{\rho}\right)_j c_j x_j \right]$$

j: denotes different materials : Contrast agent, Soft tissue, Bone which are characterized by their energy-dependent mass absorption coefficients $(\mu/\rho)_j$ and their mass density $c_j x_{j.}$

Two measurements:

Above (A) and Below (B) the K-edge

$$N_A = N_{A0} \exp\left[-\sum_j \left(\frac{\mu}{\rho}\right)_{j,A} c_j x_j \right]$$

$$N_B = N_{B0} \exp\left[-\sum_j \left(\frac{\mu}{\rho}\right)_{j,B} c_j x_j \right]$$

Iodine and Tissue mass density

If we consider two materials: Iodine and Tissue,
we can retrieve from the two measurements their mass densities

$$c_i x_i = \frac{\left(\frac{\mu}{\rho}\right)_{i,B} \ln\left[\frac{N_{A0}}{N_A}\right] - \left(\frac{\mu}{\rho}\right)_{i,A} \ln\left[\frac{N_{B0}}{N_B}\right]}{\left(\frac{\mu}{\rho}\right)_{i,B}\left(\frac{\mu}{\rho}\right)_{t,A} - \left(\frac{\mu}{\rho}\right)_{i,A}\left(\frac{\mu}{\rho}\right)_{t,B}}$$

$c_i t_i =$

$$c_t x_t = \frac{\left(\frac{\mu}{\rho}\right)_{i,B} \ln\left[\frac{N_{A0}}{N_A}\right] - \left(\frac{\mu}{\rho}\right)_{i,A} \ln\left[\frac{N_{B0}}{N_B}\right]}{\left(\frac{\mu}{\rho}\right)_{i,B}\left(\frac{\mu}{\rho}\right)_{t,A} + \left(\frac{\mu}{\rho}\right)_{i,A}\left(\frac{\mu}{\rho}\right)_{t,B}}$$

K-edge Imaging

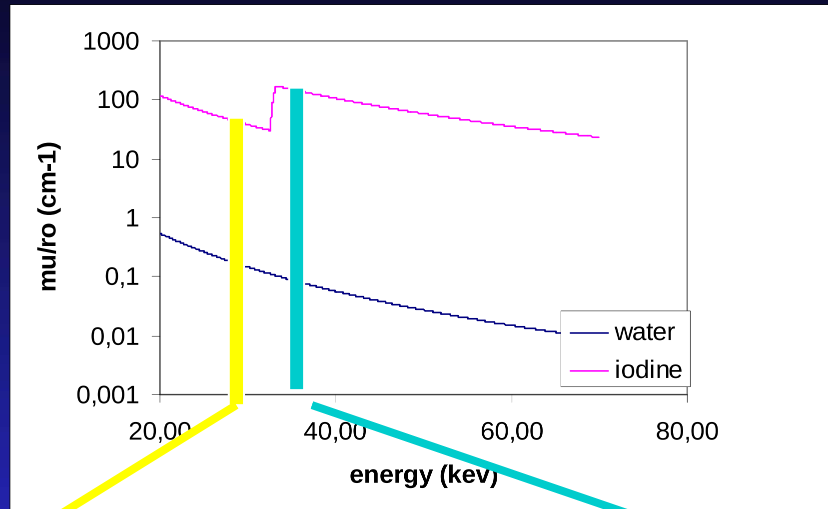

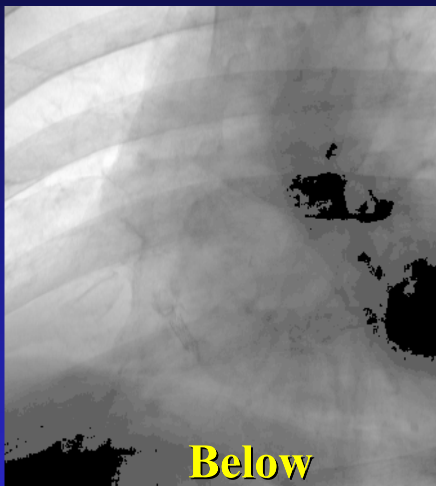

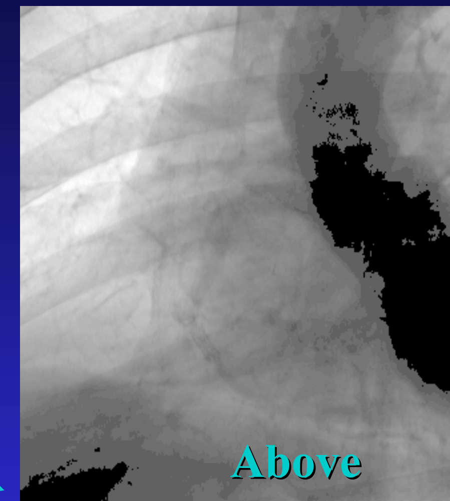

Detectable concentration limits (I and Gd)

Table 2. Experimental results: minimum detectable concentration of iodine or gadolinium (defined as SNR of 3)—comparison of K-edge and temporal subtraction methods. Measurements performed on a Lucite phantom 16.5 cm in diameter surrounded by an aluminium ring 0.5 cm thick, with a surface radiation doseof 60 cGy (both images), detail size: 0.3 cm and beam height: 0.10 cm.

Element	Iodine	Gadolinium
K-edge method (μg ml^{-1})	185	81
Temporal subtraction at optimal energy (μg ml^{-1})	90 at 50.0 keV	58 at 50.3 keV

Beamline instrumentation for K-edge imaging

K-edge Setup

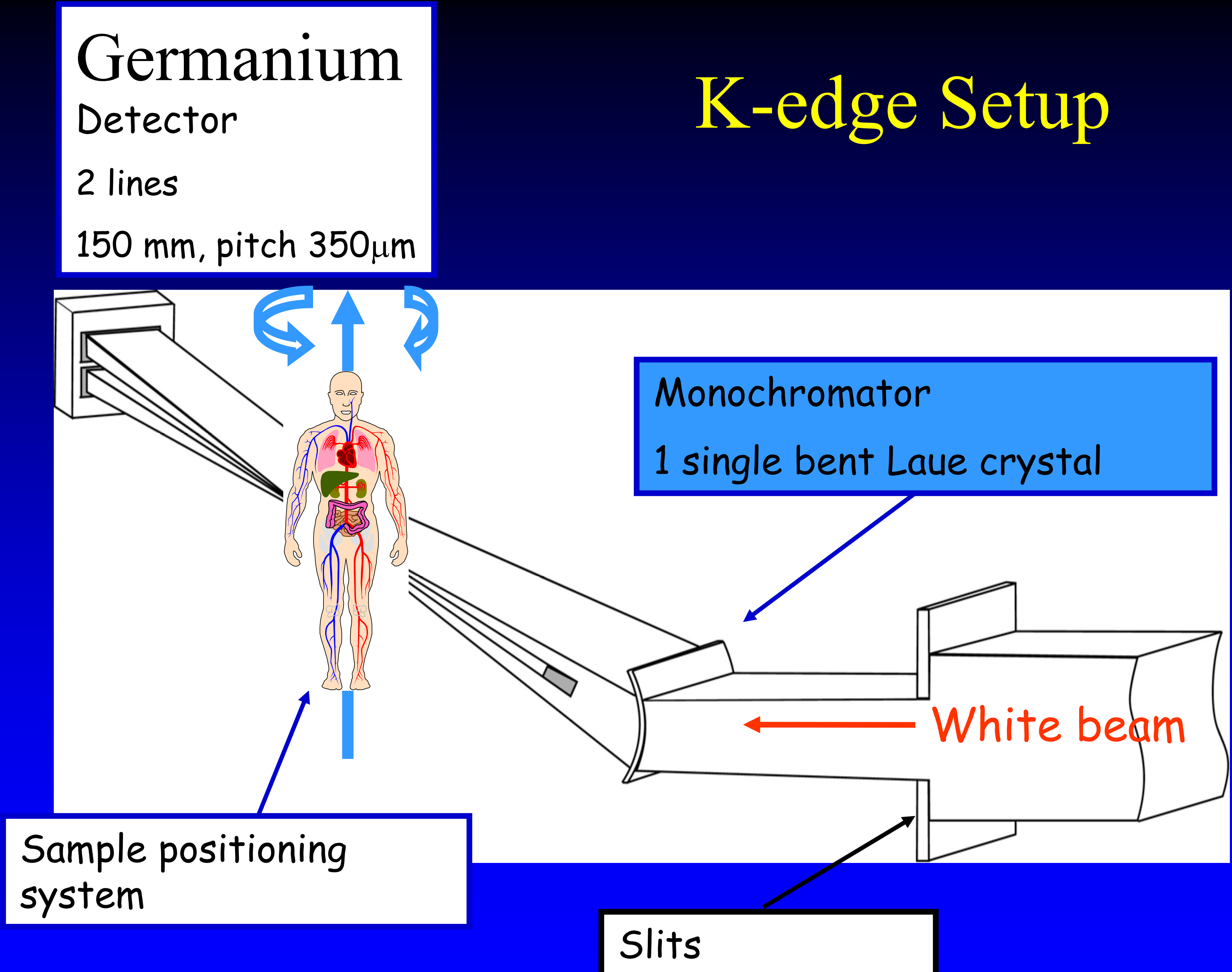
Germanium
Detector
2 lines
150 mm, pitch 350μm
Monochromator
1 single bent Laue crystal
White beam
Sample positioning system
Slits

Monochromatic energy range

The ID17 beamline has 4 monochromators

First experimental hutch (≈35 m from source)

- Fixed exit (Laue-Laue), first hutch: 30-80 keV, $\Delta E/E \approx 0.1\%$

Second experimental hutch (≈145 m from source)

- Fixed exit (Laue-Laue), second hutch: 20-88 keV, $\Delta E/E \approx 0.1\%$
- Single bent Laue crystal, second hutch: 20-80 keV, $\Delta E/E \approx 0.1\%$
- Fixed exit (multilayer), second hutch: 7-35 keV, $\Delta E/E \approx 1\%$

Exploitable element table (at ID17)

Element	K 1s
26 Fe	7112
27 Co	7709
28 Ni	8333
29 Cu	8979
30 Zn	9659
31 Ga	10367
32 Ge	11103
33 As	11867
34 Se	12658
35 Br	13474
36 Kr	14326
37 Rb	15200
38 Sr	16105
39 Y	17038
40 Zr	17998
41 Nb	18986
42 Mo	20000
43 Tc	21044
44 Ru	22117
45 Rh	23220
46 Pd	24350
47 Ag	25514

Element	K 1s	L_1 2s
48 Cd	26711	
49 In	27940	
50 Sn	29200	
51 Sb	30491	
52 Te	31814	
53 I	33169	
54 Xe	34561	
55 Cs	35985	
56 Ba	37441	
57 La	38925	
58 Ce	40443	
59 Pr	41991	
60 Nd	43569	7126
61 Pm	45184	7428
62 Sm	46834	7737
63 Eu	48519	8052
64 Gd	50239	8376
65 Tb	51996	8708
66 Dy	53789	9046
67 Ho	55618	9394
68 Er	57486	9751
69 Tm	59390	10116
70 Yb	61332	10486

Element	K 1s	L_1 2s	L_2 $2p_{1/2}$	L_3 $2p_{3/2}$
71 Lu	63314	10870	10349	9244
72 Hf	65351	11271	10739	9561
73 Ta	67416	11682	11136	9881
74 W	69525	12100	11544	10207
75 Re	71676	12527	11959	10535
76 Os	73871	12968	12385	10871
77 Ir	76111	13419	12824	11215
78 Pt	78395	13880	13273	11564
79 Au	80725	14353	13734	11919
80 Hg	83102	14839	14209	12284
81 Tl	85530	15347	14698	12658
82 Pb	88005	15861	15200	13035
83 Bi	90524	16388	15711	13419

K-shell from Fe (Z=26) to Bi (Z=83)

L-shell from Nd (Z=60) to Bi (Z=83)

"Electron binding energies in eV", X-ray data booklet, http://xdb.lbl.gov/

K-edge imaging

Applications:
Clinical coronary artery

K-edge Imaging

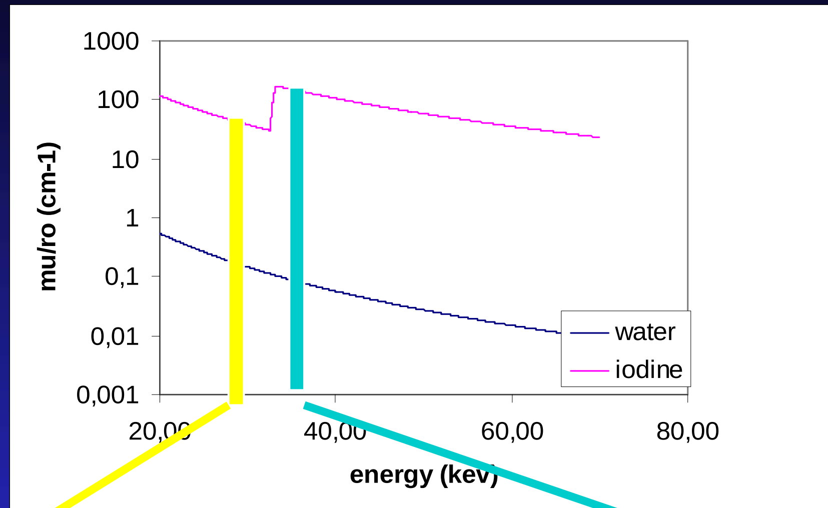

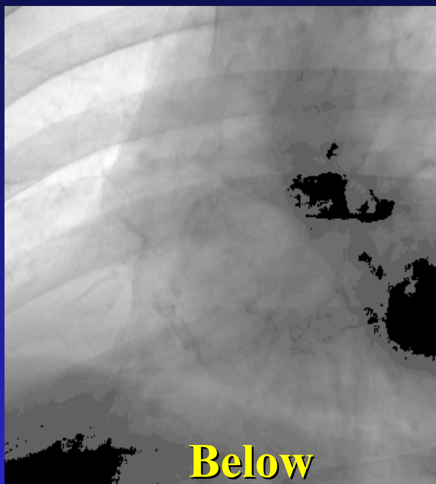

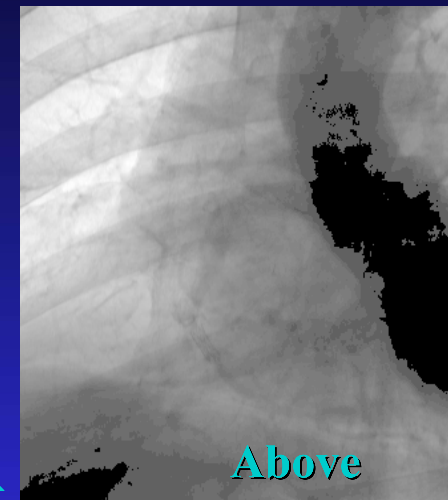

B. Bertrand et al. Europ. Heart J., 2005 26: 1284-1291

K-edge imaging

Applications:
In-vivo bronchography

In-vivo imaging of airways and lungs filled with Xe in rabbit for asthma studies

Aim: understanding origin and physiology of an asthma crisis for finding better treatments

Projection image

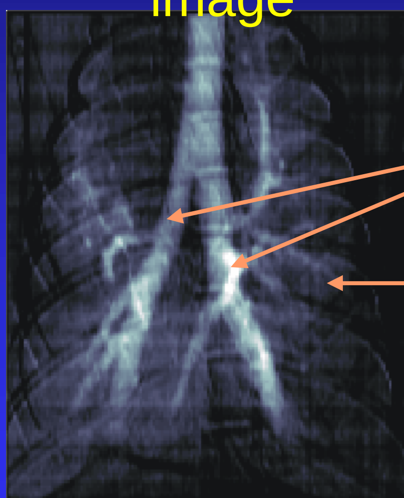

CT image

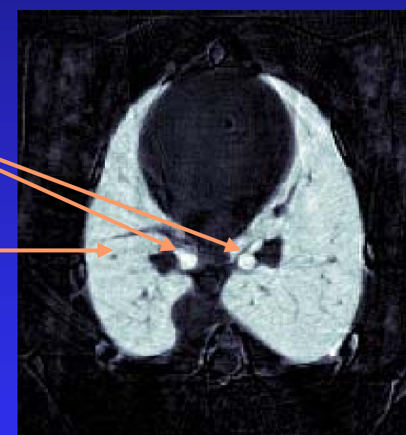

Airways

Lung tissue

- Xe in the bronchial tree
- Pixel size 0.35x0.35mm
- Maximum image width 15.0 cm

- Xenon in lung tissue (air spaces)
- Voxel size $0.35 \times 0.35 \times 0.7 mm^3$
- Cross sections of the airways
- Max 1 image /s

Bayat et al. Phys Med Biol 46: 3287 - 3299, 2001

Experimental set-up

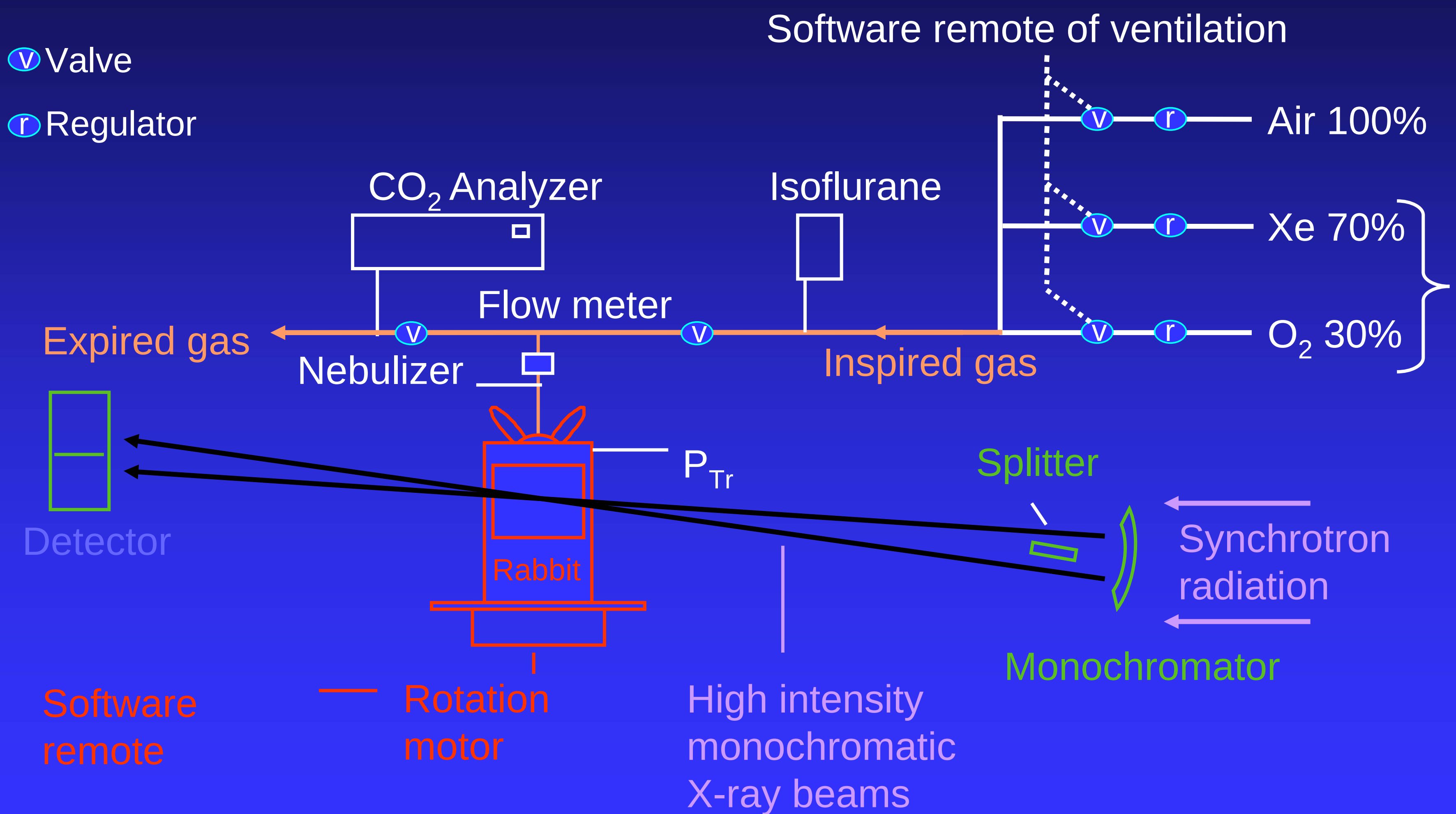

Porra et al. J Appl Physiol 96: 1899 -1908, 2004

Imaging of constriction of single airways after histamine inhalation

Baseline | 6 min | 24 min | 64 min

Inspiration

Histamine aerosol

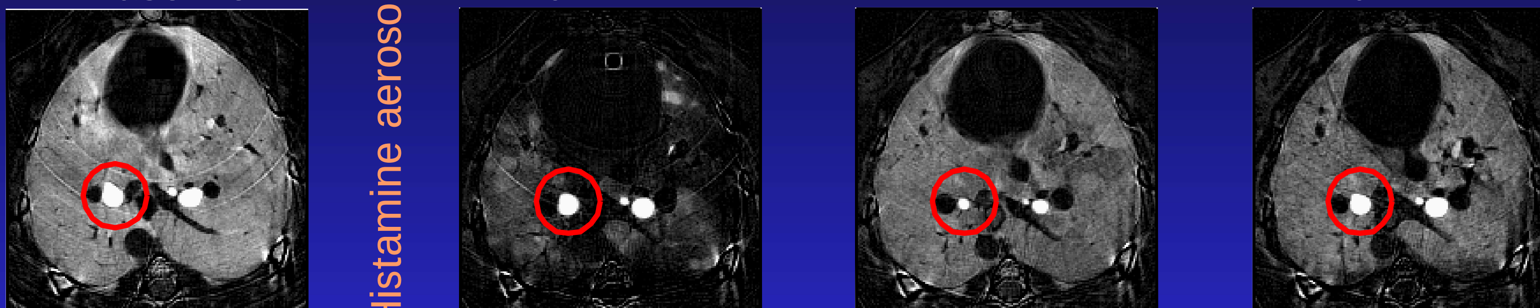

4.4mm | 4.2mm | 2.3mm | 3.6 mm

↔ 1cm

Diameters of circled airways

Airway cross-sectional area (N=6)

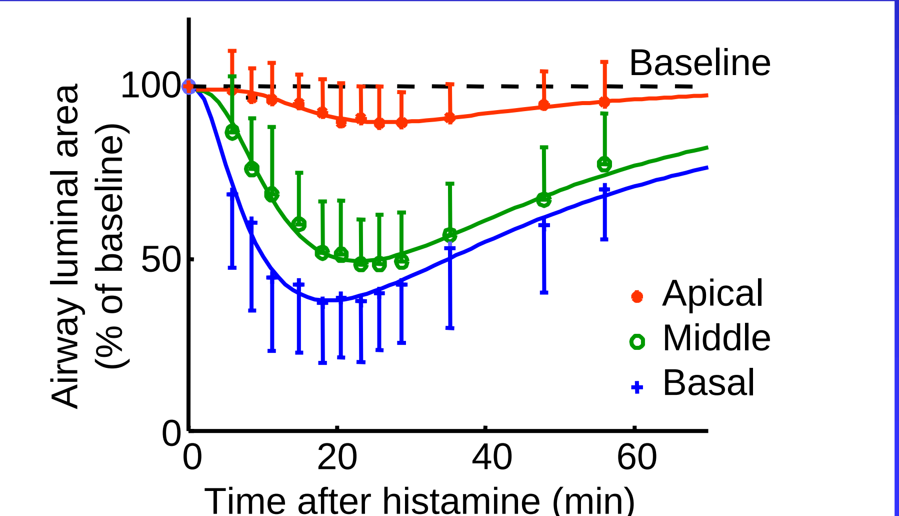

- Spontaneous recovery starts after 20 min

K-edge imaging

Applications:
Brain perfusion measurements

Brain perfusion measurements

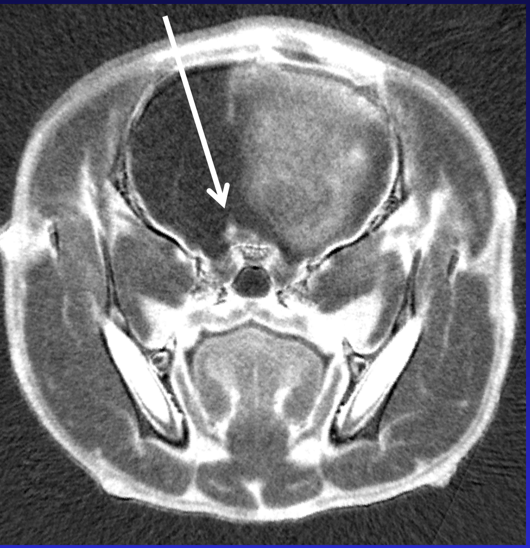

- **Contrast agent is injected at t=0**
- **CT slices are acquired at fixed intervals (1-5 minutes)**
- **Two beams bracketing the contrast agent K-edge (Iodine: 33.17 keV) are focused on sample**
- **Images are logarithmically subtracted to extract the concentration maps**

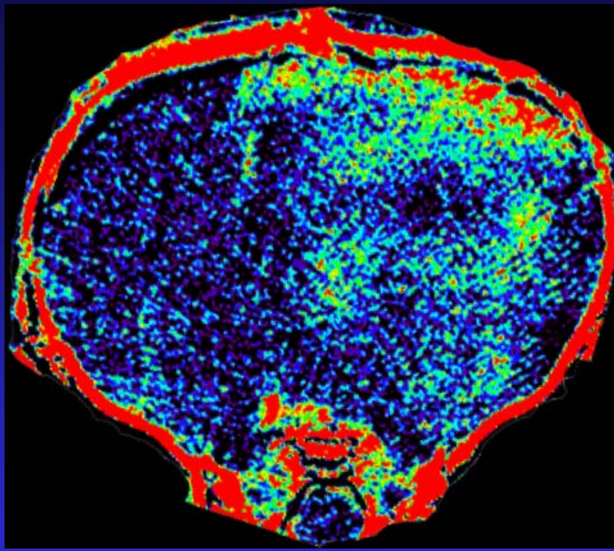

CBV map

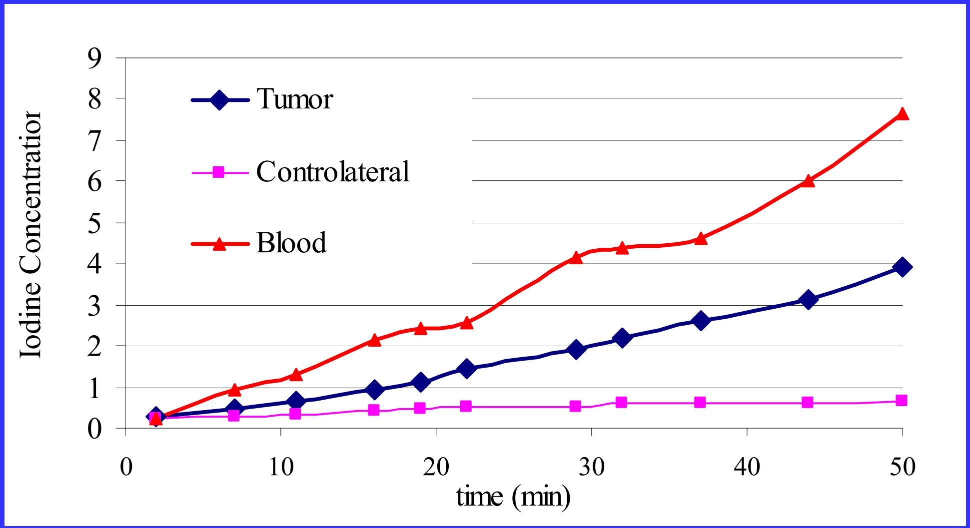

Iodine concentration variation in several ROIs: tumoral zone, controlateral brain, blood

J-F Adam, et al. *J. Cerebral Blood Flow & Met. (2005) 25, 145−153*

K-edge imaging

Applications (material science/cultural heritage): *Looking under paintings*

Visible light (photo) of a test canvas

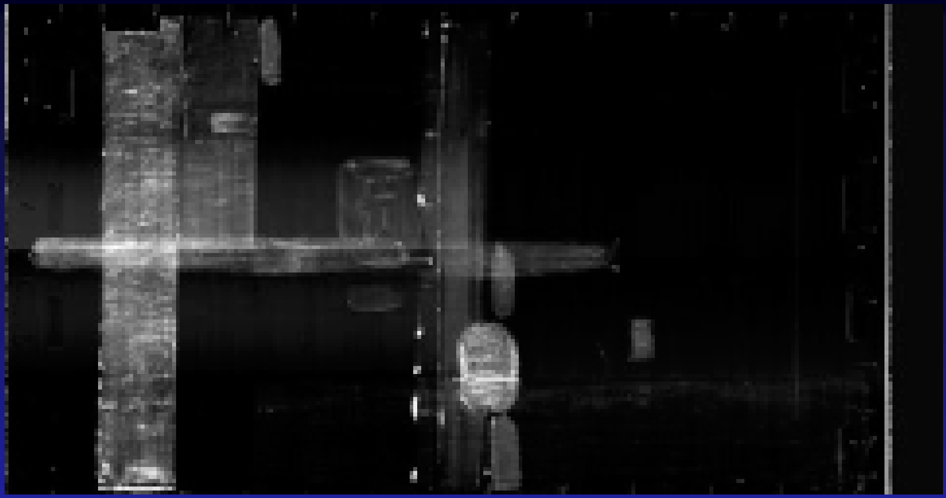

Lead (white) K-edge image (88.005 keV)

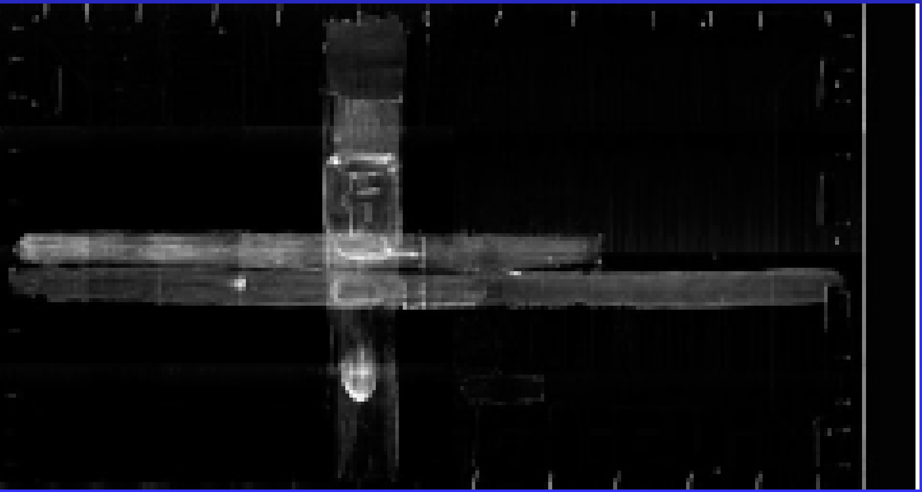

Barium (red) K-edge image (37.441 keV)

- Colours can be analyzed individually
- Underlying layers/paintings can be visualized
- “Errors”, fakes, or modifications can be detected

The
Temporal subtraction imaging technique

The temporal subtraction imaging

- Subtraction of two images, performed at the same energy (E_γ) typically above the edge of an element, before and after the injection of the contrast agent.

- It can be applied when motion artifacts are small (brain, spine, legs, or phantoms).

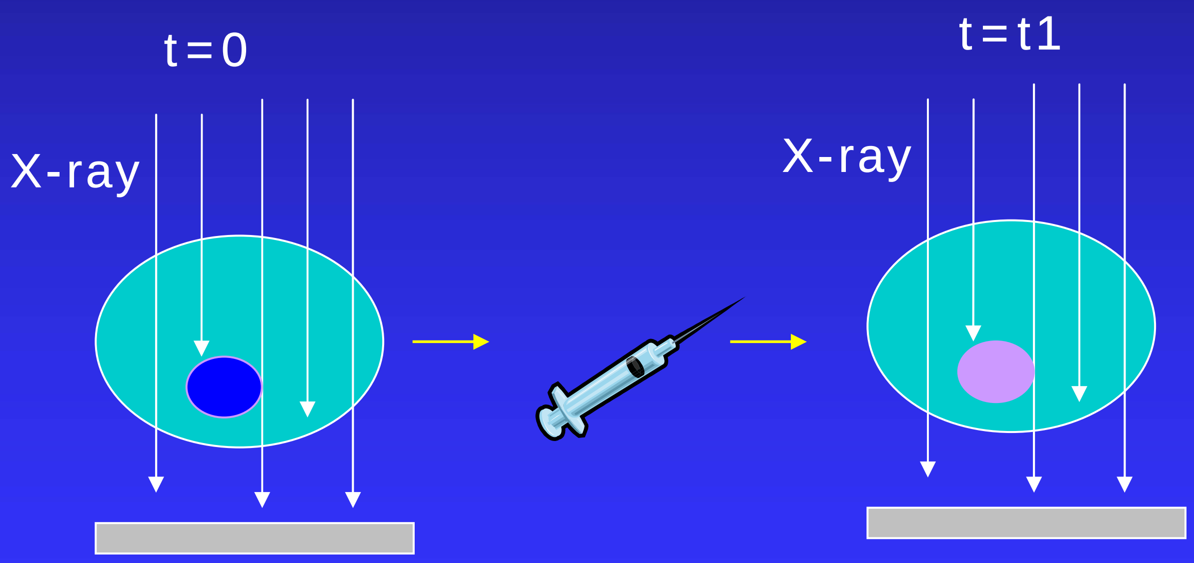

Reference image **Image with contrast agent**

- The linear attenuation coefficient maps ($\mu_{E\gamma\text{-}t1}$ and $\mu_{E\gamma\text{-}t2}$) are obtained at times t_1 and t_2, before and after the addition of the element M_2 to the principal medium M_1.

(ρ_M=density, $a_{Ei\text{-}Mk}$ =mass attenuation coefficients $(\mu/\rho_{Mk})_{E_i}$ of the material M_k at the energy E_i)

$$\begin{pmatrix} \mu_{E_\gamma t_1} \\ \mu_{E_\gamma t_2} \end{pmatrix} = \begin{pmatrix} a_{E_\gamma M_1} & 0 \\ a_{E_\gamma M_1} & a_{E_\gamma M_2} \end{pmatrix} \begin{pmatrix} \rho_{M_1} \\ \rho_{M_2} \end{pmatrix}$$

Attenuation coefficients

$$\begin{pmatrix} \rho_{M_1} \\ \rho_{M_2} \end{pmatrix} = \frac{1}{|A|} \begin{pmatrix} a_{E_\gamma M_2} & 0 \\ -a_{E_\gamma M_1} & a_{E_\gamma M_1} \end{pmatrix} \begin{pmatrix} \mu_{E_\gamma t_1} \\ \mu_{E_\gamma t_2} \end{pmatrix}$$

Element concentrations

Interaction of X-rays with tissues (pictorial)

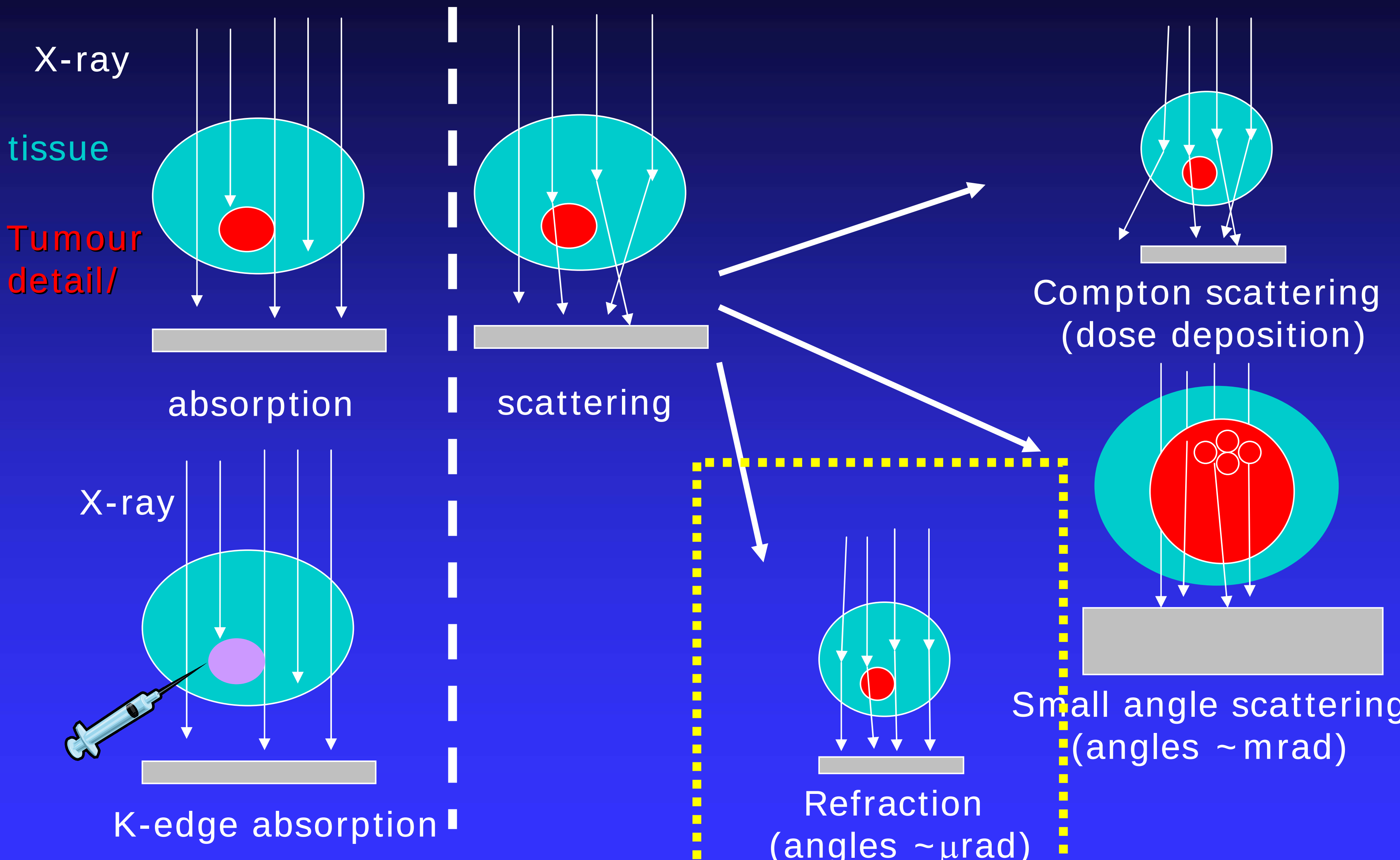

http://detserv1.dl.ac.uk/Herald/xray_history.htm

Refraction contrast or "phase contrast"

There are several phase sensitive technique in the X-ray regime:

- Simple (free) propagation (P. Cloetens' presentation)
- Analyser based imaging (Diffraction Enhanced Imaging –DEI)
- Interferometry *(Takeda et al. Radiol. 2000; 214:298-301)*

  (Pfeiffer F, et al, Phys Rev Lett. 2005 29;94(16):164801)

Analyser Based Imaging (ABI)

Analyzer:
acts as a perfect and
extremely narrow slit

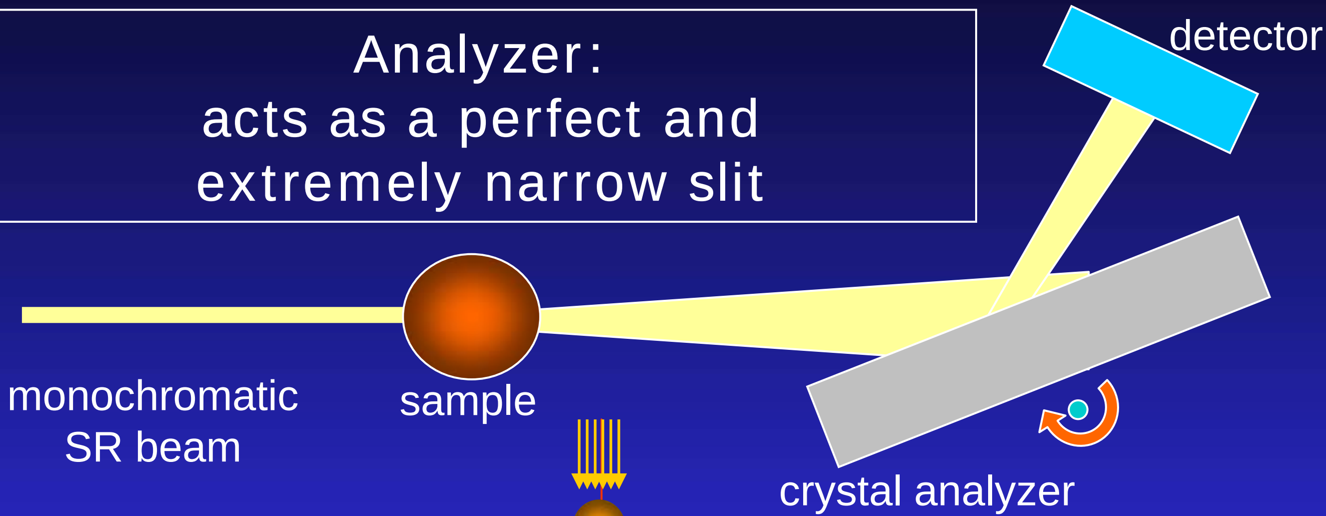

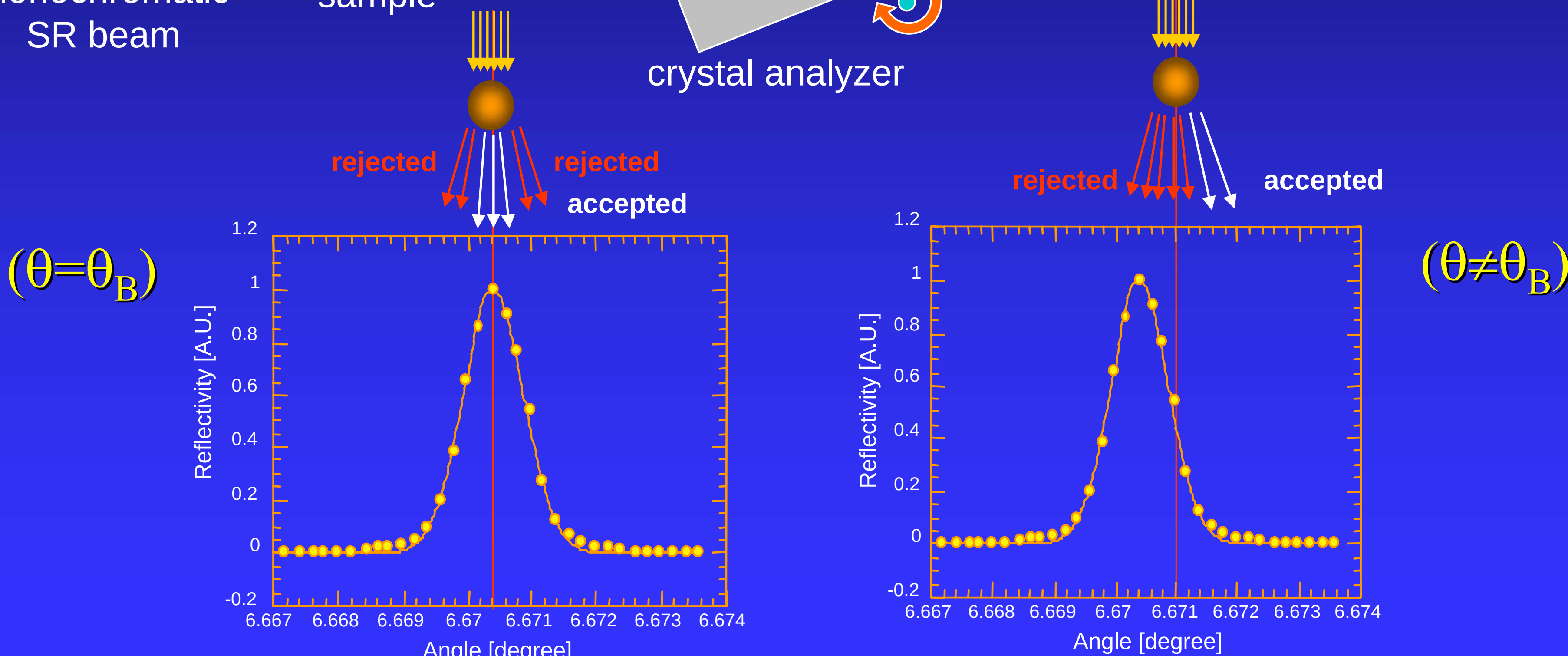

ABI on cylindrical plastic fibers

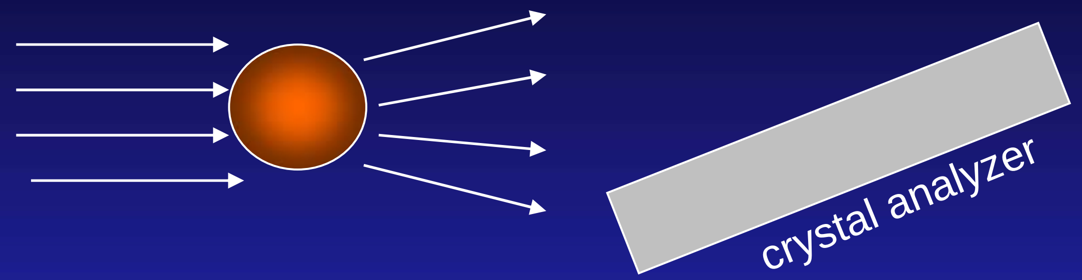

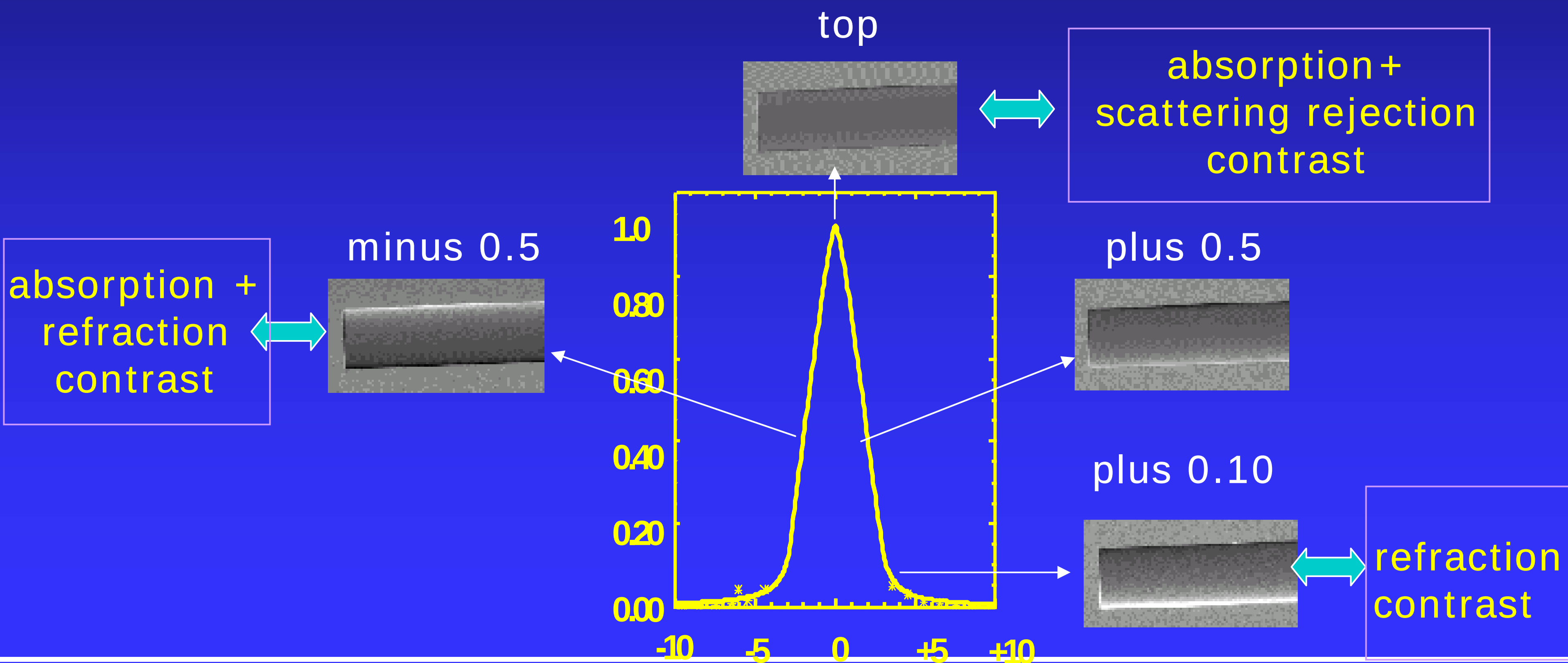

From R. Lewis et al. SPIE 2002

Diffraction Enhanced Imaging: an algorithm for ABI

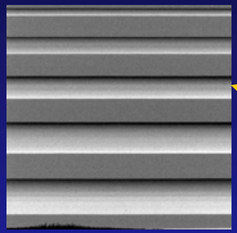

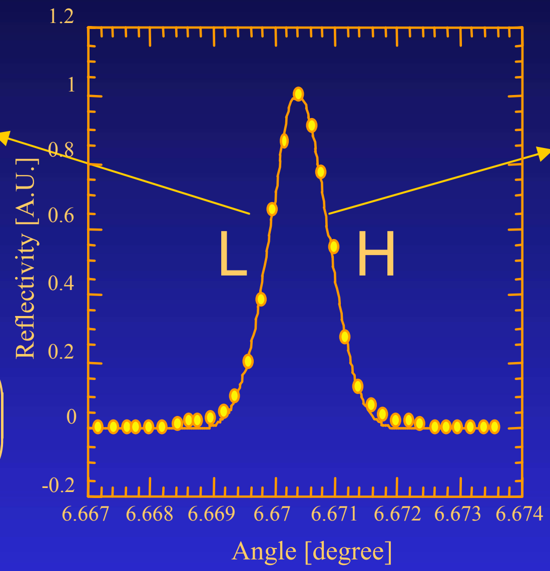

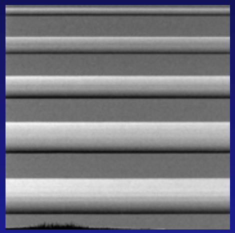

$$I_L = I_R\left(R(\Theta_L) + \frac{\partial R}{\partial \Theta}(\Theta_L)\Delta\Theta_z\right)$$

$$I_H = I_R\left(R(\Theta_H) + \frac{\partial R}{\partial \Theta}(\Theta_H)\Delta\Theta_z\right)$$

I_R = apparent absorption image

$\Delta\Theta_Z$ = refraction image in the plane of the object

$$I_R = \frac{I_L \cdot \left.\frac{dR}{d\Theta}\right|_{\Theta_H} - I_H \cdot \left.\frac{dR}{d\Theta}\right|_{\Theta_L}}{R(\Theta_L)\cdot \left.\frac{dR}{d\Theta}\right|_{\Theta_H} - R(\Theta_H)\cdot \left.\frac{dR}{d\Theta}\right|_{\Theta_L}}$$

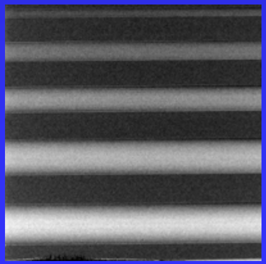

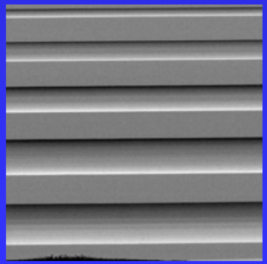

$$\Delta\Theta_Z = \frac{I_H \cdot R(\Theta_L) - I_L \cdot R(\Theta_H)}{I_L \cdot \left.\frac{dR}{d\Theta}\right|_{\Theta_H} - I_H \cdot \left.\frac{dR}{d\Theta}\right|_{\Theta_L}}$$

LOCAL & STATISTICAL METHOD for DEI:

Algorithm based on local rocking curve in each pixel of the detector

- Integrated absorption: $I_{abs} = M_{0,obj} / M_{0,ref}$
- Maximum absorption: $I_m = m_{obj} / m_{ref}$.
- Integrated refraction: $\Delta\theta_0 = \theta_{0,obj} - \theta_{0,ref}$ (µrad)
- Ultra Small Angle X-ray Scattering: $\sigma_u = (\sigma_{obj}^2 - \sigma_{ref}^2)^{1/2}$ (µrad)

Standard deviation

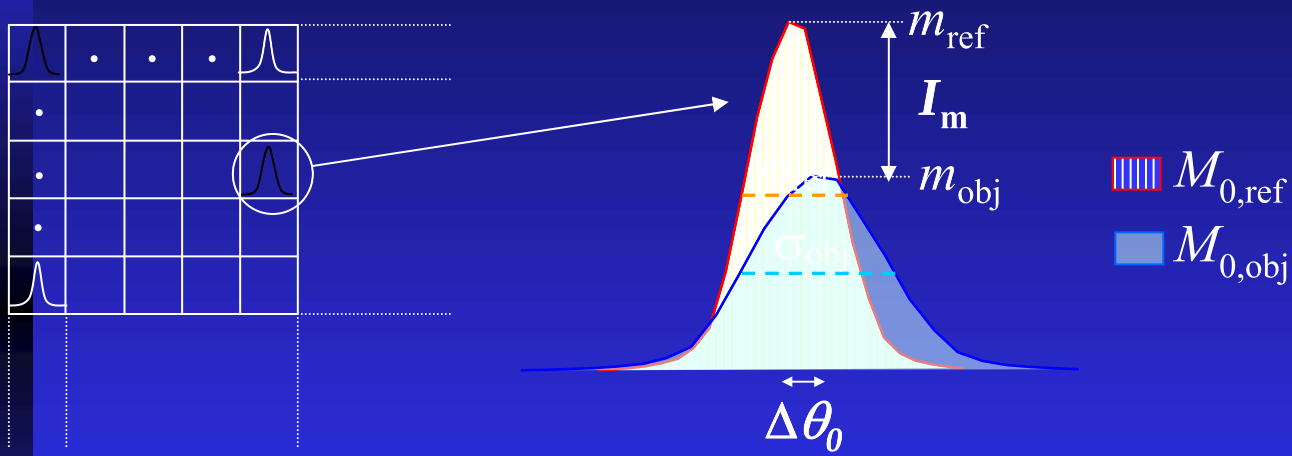

1 mm tumor like mass - 24 image series - 18 keV:

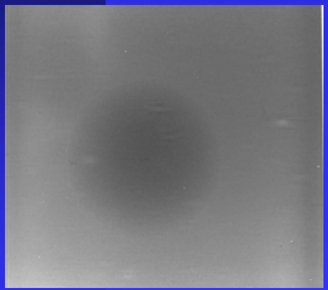

Integrated absorption I_{abs}

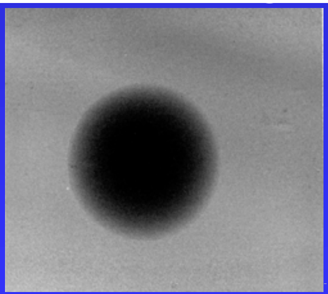

Maximum absorption I_m

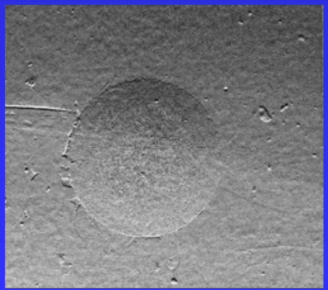

Integrated refraction $\Delta\theta_0$

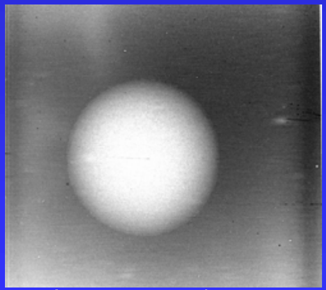

Ultra Small Angle X-ray Scattering σ_u

*E. Pagot et al, Appl. Phys. Lett., **82**, 20 (2003)*

Rocking curve width Si (333)

~ 3.0 μrad @ 25 keV

~ 1.3 μrad @ 50 keV

~ 0.9 μrad @ 60 keV

Note: how much is 1 μrad??

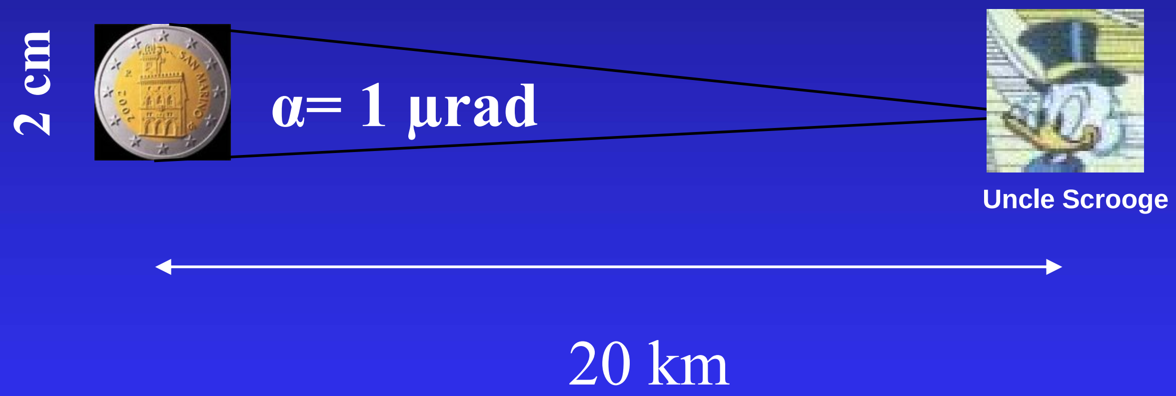

Highly stable set-up is needed!!

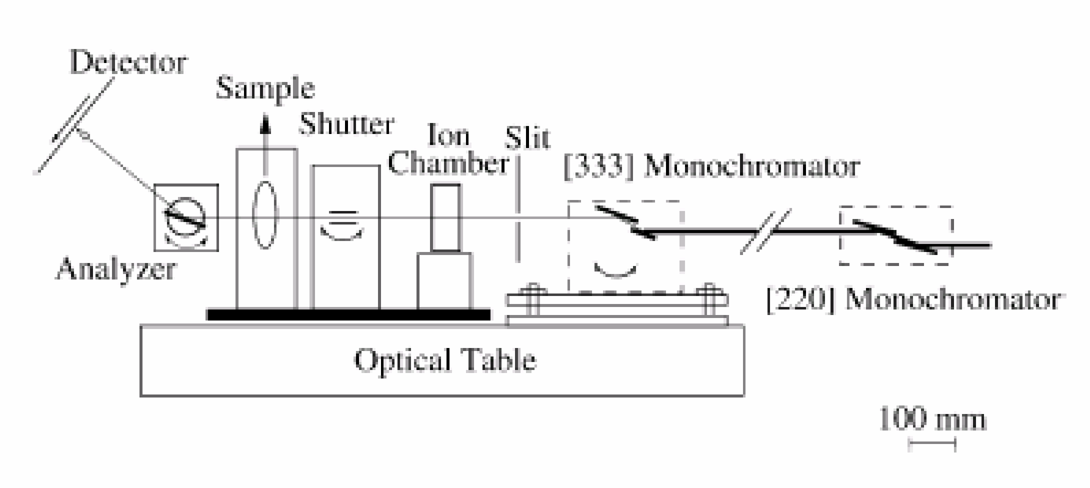

Instrumentation

Zhong, NIMA (2000)

- **High stable set-up Si(555)**
- **E=15-60 keV**
- **Image plates**

- **Fixed exit set-up Si(333)**
- **E=20-60 keV**
- **Taper optics Frelon camera**

analyser

sample

Pre-
monochromator

beam

A. Bravin, J Phys D: Appl. Phys.36, A-24-29 (2003)

Analyser-based Imaging: Mammography

Application: Mammography

Motivations

- **The improvement of sensitivity in mammography is of crucial importance (10% of tumors are missed)**
- **Low absorption contrast generated by breast cancer and by small tumor masses**
- **Strong diffuse scattering which reduces the image contrast**
- **High radiation sensitivity – low dose imaging needed**

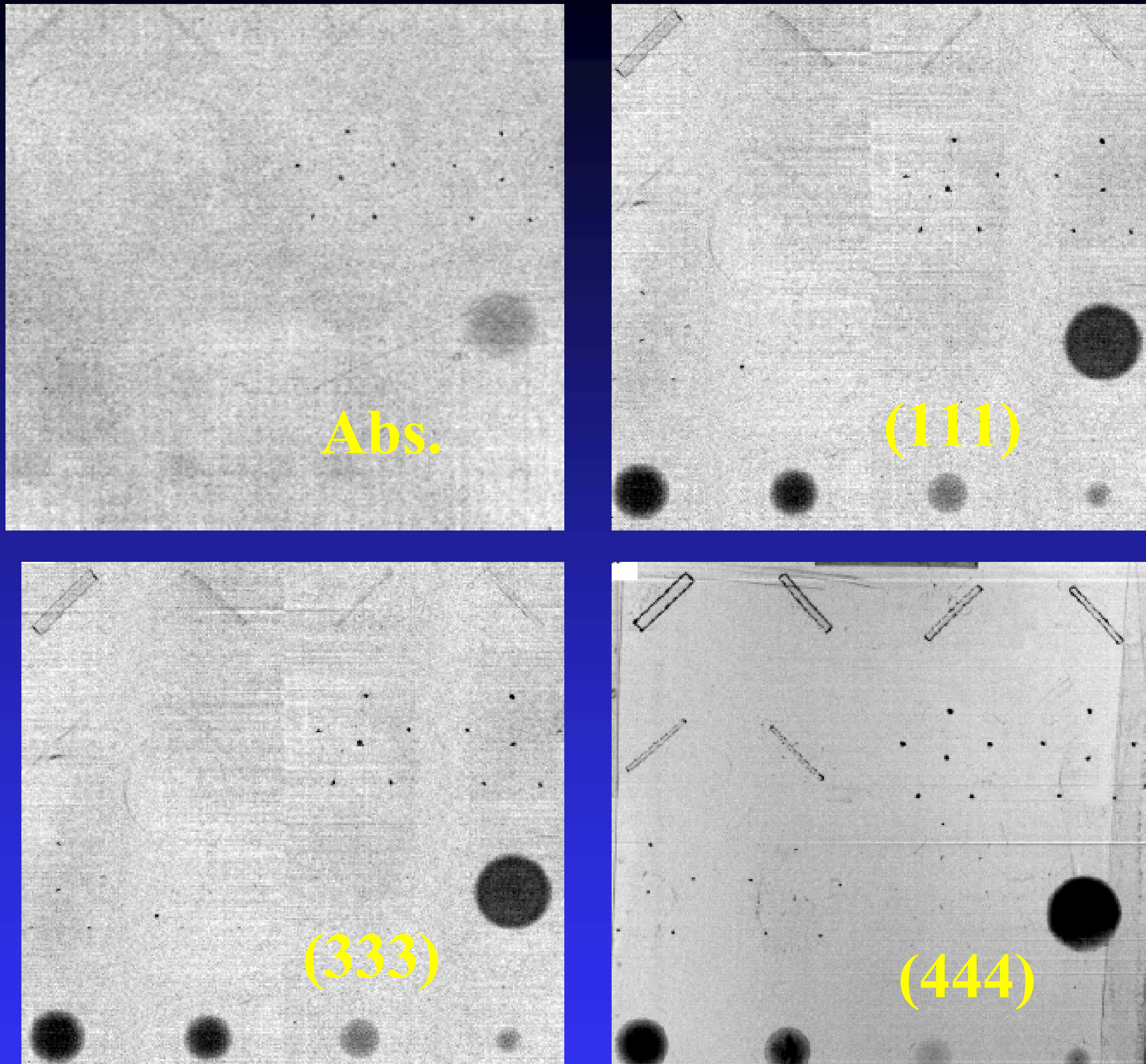

ACR mammographic phantom

21-25 keV

• The contrast shows an improvement as large as one order of magnitude when moving from (111) to (333) or (444) reflections

• This adds to the one order of magnitude improvement typical of ABI on (111), as compared to transmission imaging

L. Rigon et al. Proc. SPIE vol. 4682, 2002

Carcinoma Medullare

- 1 Siemens Mammomat 3000 -23 kVp- 5.6 mAs; MGD=0.4 mGy

- 2 ABI 25 keV minus 0.7 µrad. Si(333); MGD= 0.6 mGy

- 3 Histology

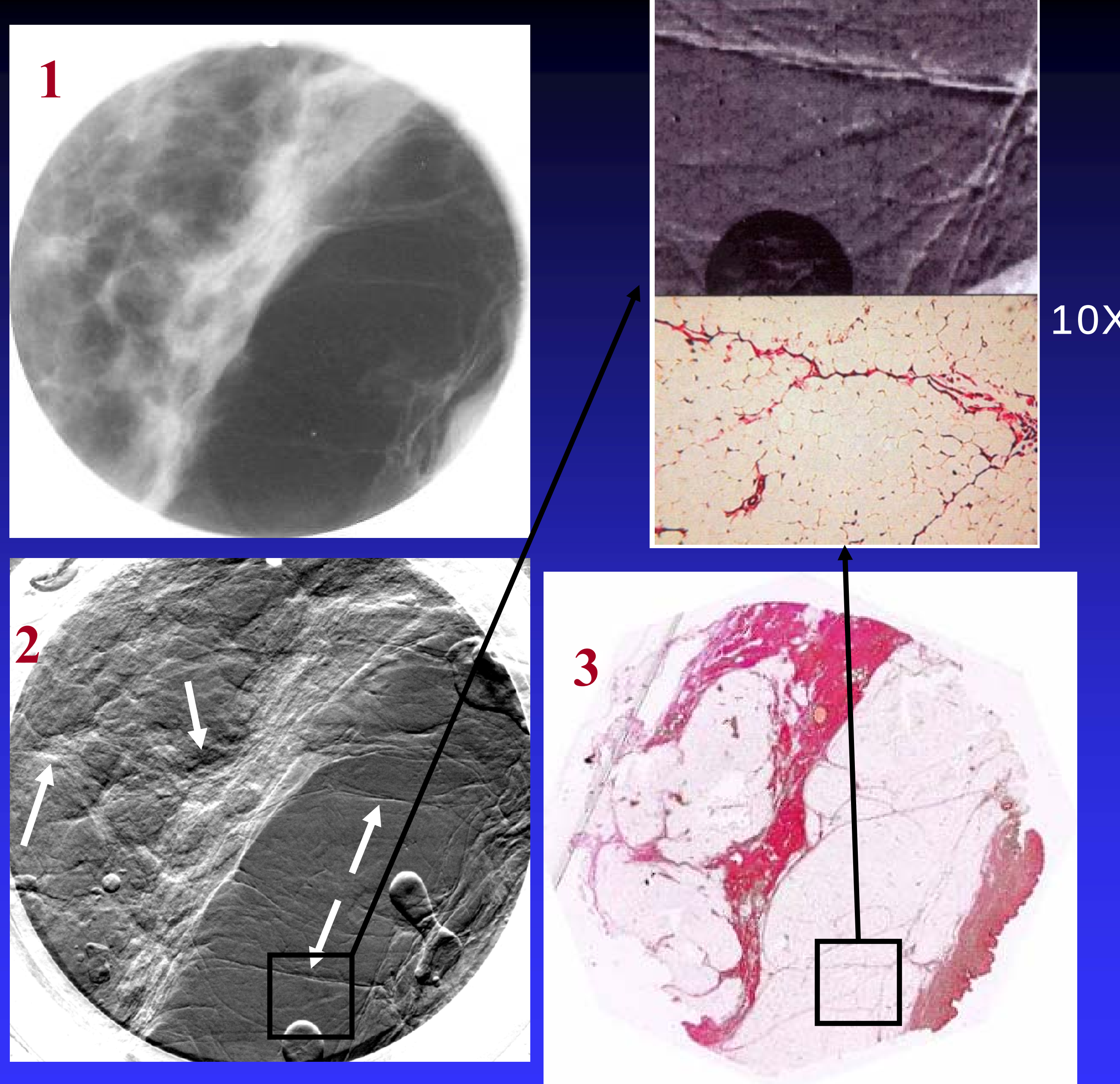

Keyriläinen et al. European Journal of Radiology 53, 226-237 (2005)

Analyser-based Imaging:
Bone and cartilage

Why focusing on cartilage joint diseases?

Osteoarthritis (OA) is one of the leading causes of disability; people with OA usually have joint **pain** and **limited movement** (stiffness)

Cartilage degeneration process – Collins grading system (Collins, 1949)

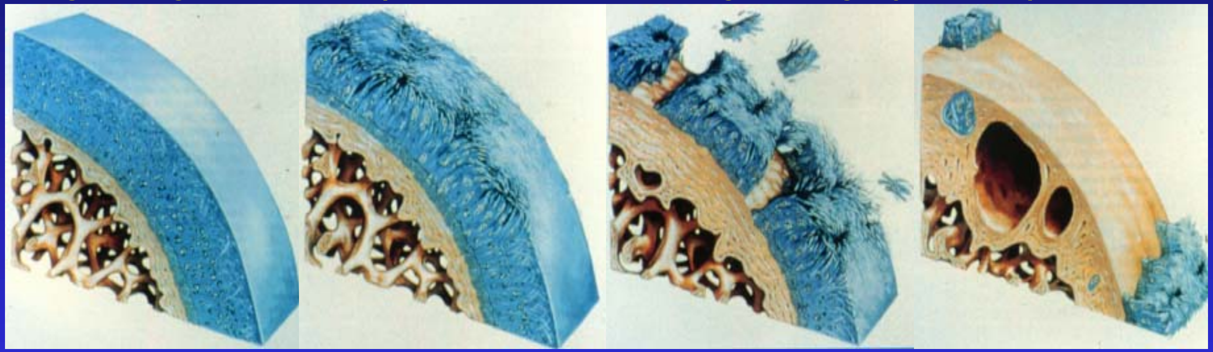

OA affects approximately 12% of the population in the seven major pharmaceutical markets (USA, Japan, France, Germany, Italy, Spain, and the UK)

http://www.marketresearch.com/map/prod/843319.html

As OA presently has no cure, so far physician treatment strategies focus on treating the disease symptoms with minimal side effects

Hip - ABI vs conventional techniques

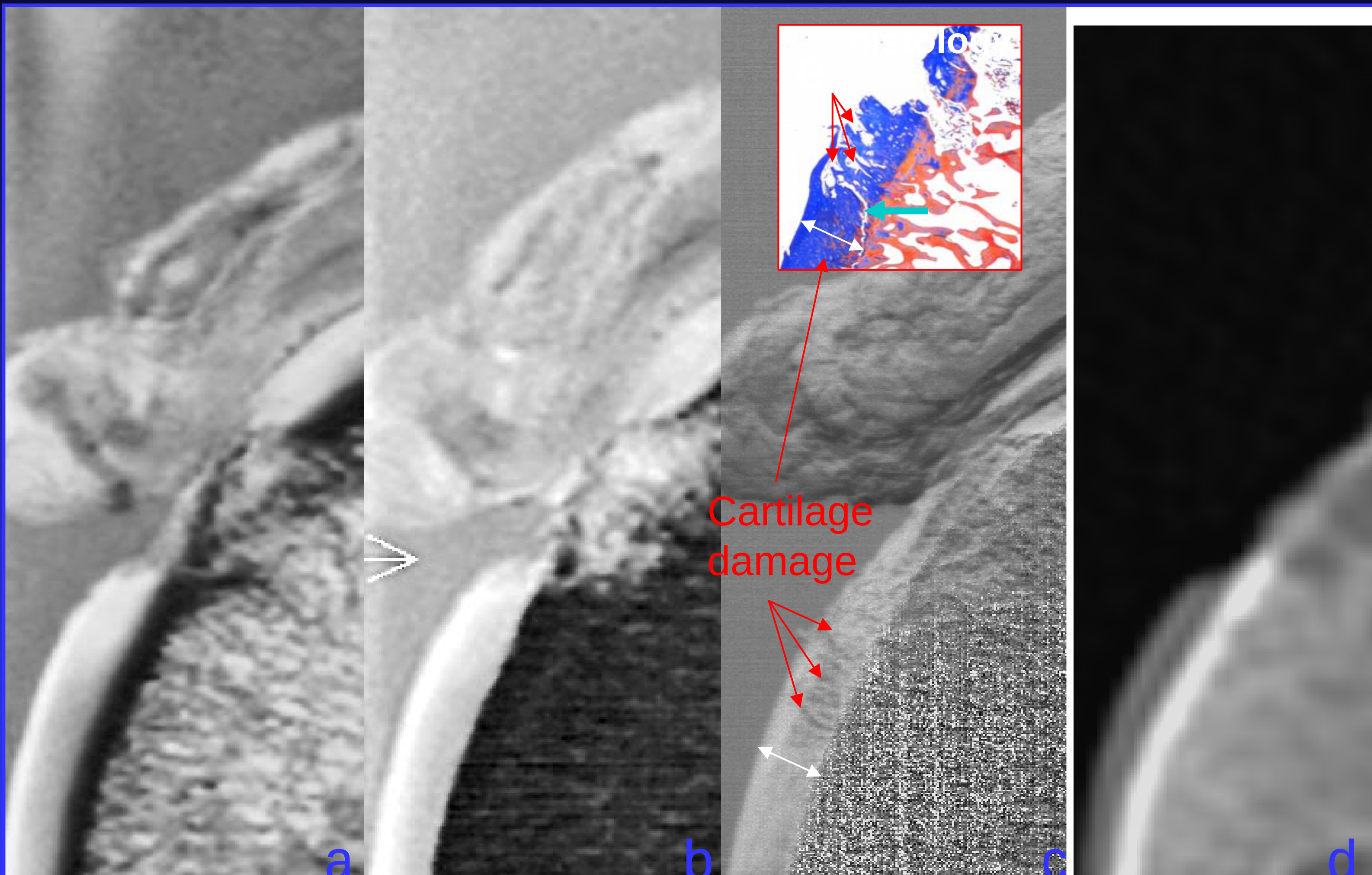

MRI >5h | MRI >5h | **DEI** (Refraction Im.) | Conventional CT

Despite (c) is a projection image structural damage of cartilage is displayed that is invisible in MRI and CT

A. Wagner *et al.*,"Options and Limitations of Joint Cartilage Imaging: DEI in Comparison to MRI and Sonography," Nucl. Instr. Meth. A **548**, 47-53 (2005)

Hip: ABI-CT vs histology

Comparison of CT ABI and histology

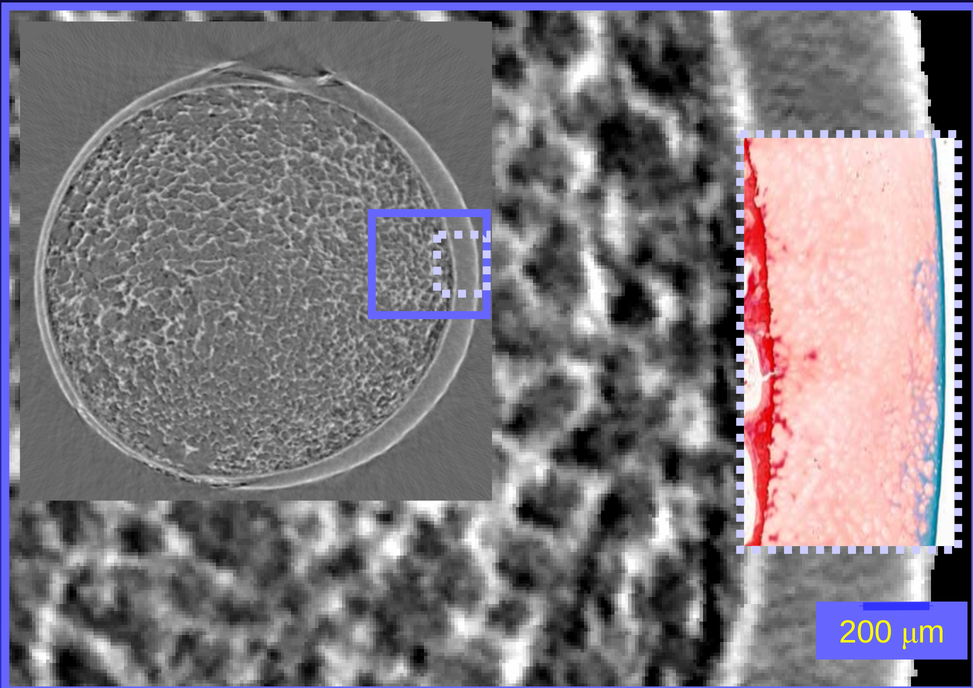

ABI-CT images perfectly match histological cuts

Human hip
50 keV Si(333)
-50%

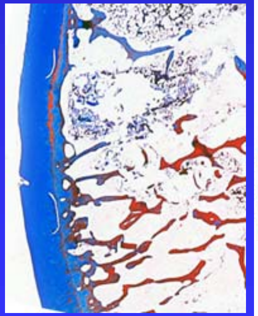

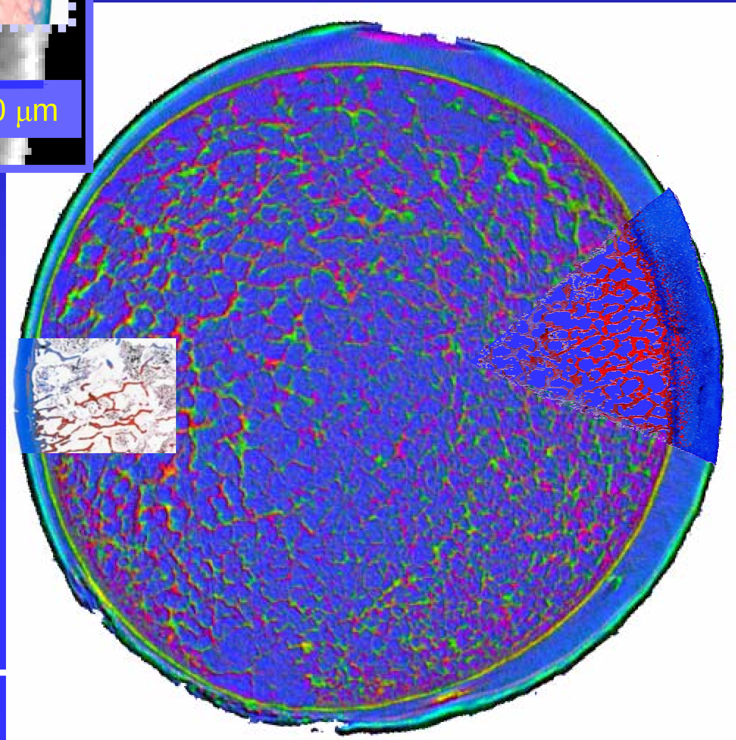

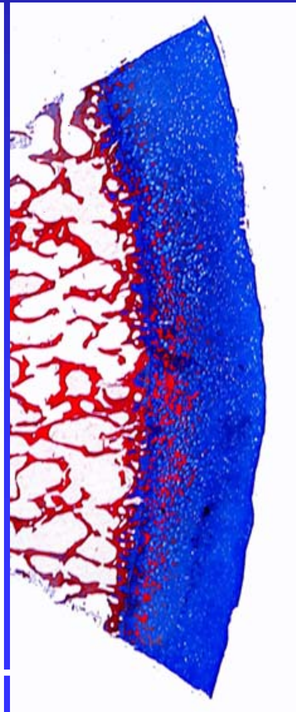

Combination of Analyser-based Imaging and Propagation

Combining Phase Propagation and ABI

PHASE PROPAGATION IMAGING

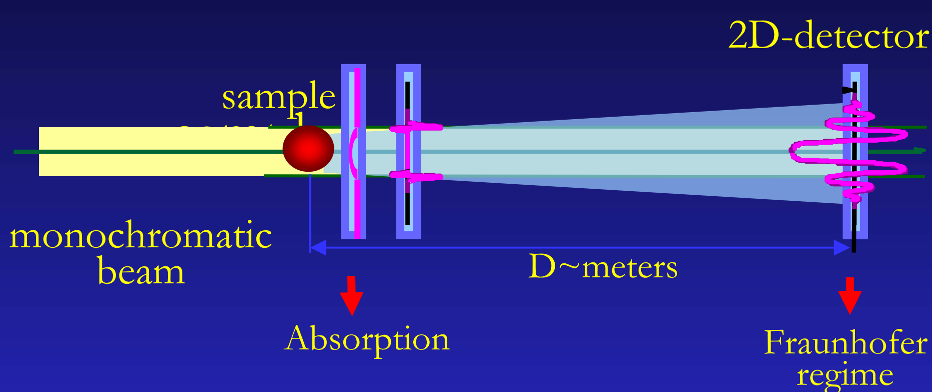

PPI sensitive to $\nabla^2 \varphi$
(2-dimensional)

ANALYSER BASED IMAGING

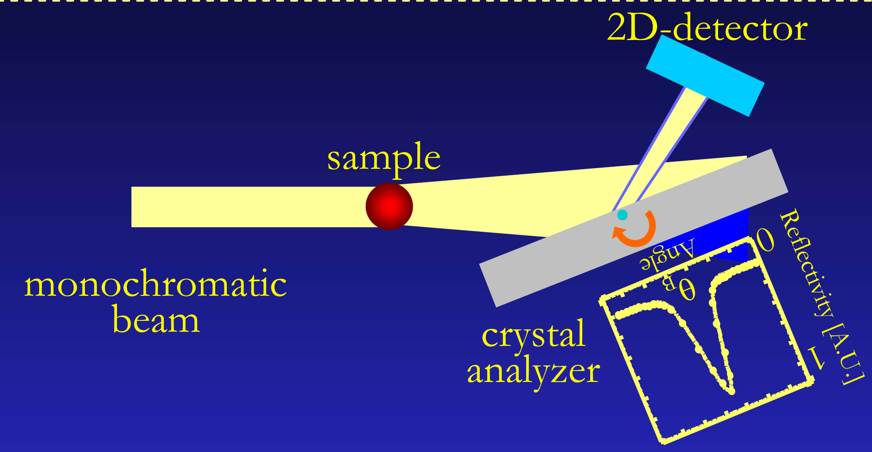

ABI sensitive to $\nabla \varphi$ (in the diffraction direction)
(1-dimensional)

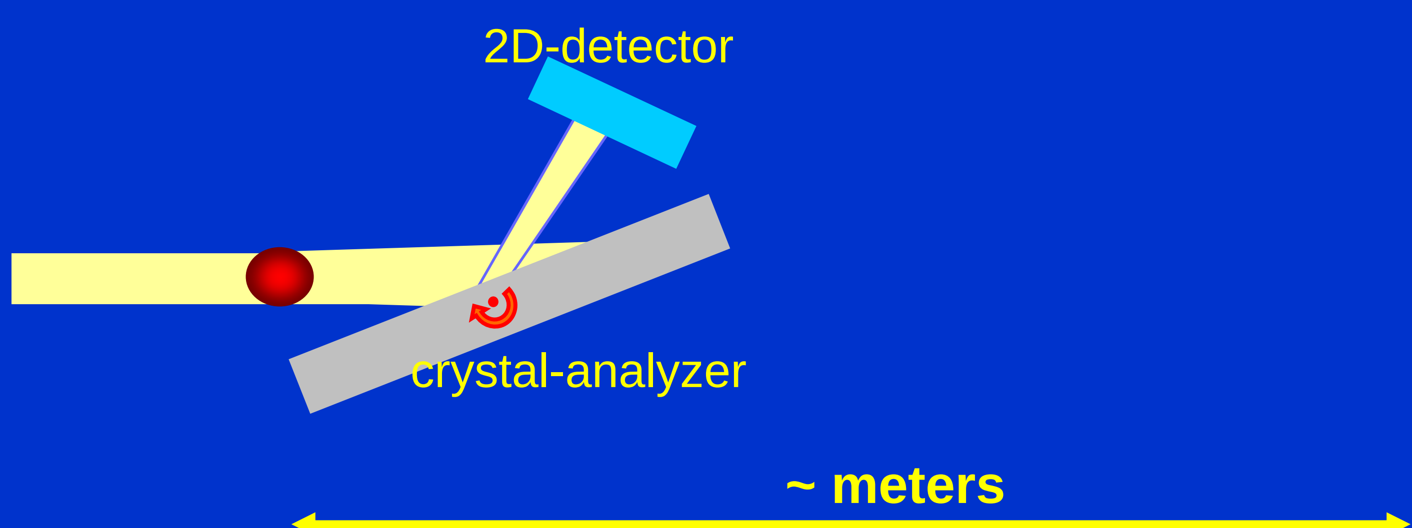

Results of this “Hybrid mode” imaging (HI)

25keV, Si(111)

sample-analyzer distance=5.6m

Wire profiles in PPI (a), ABI (b) and HI (c) imaging techniques

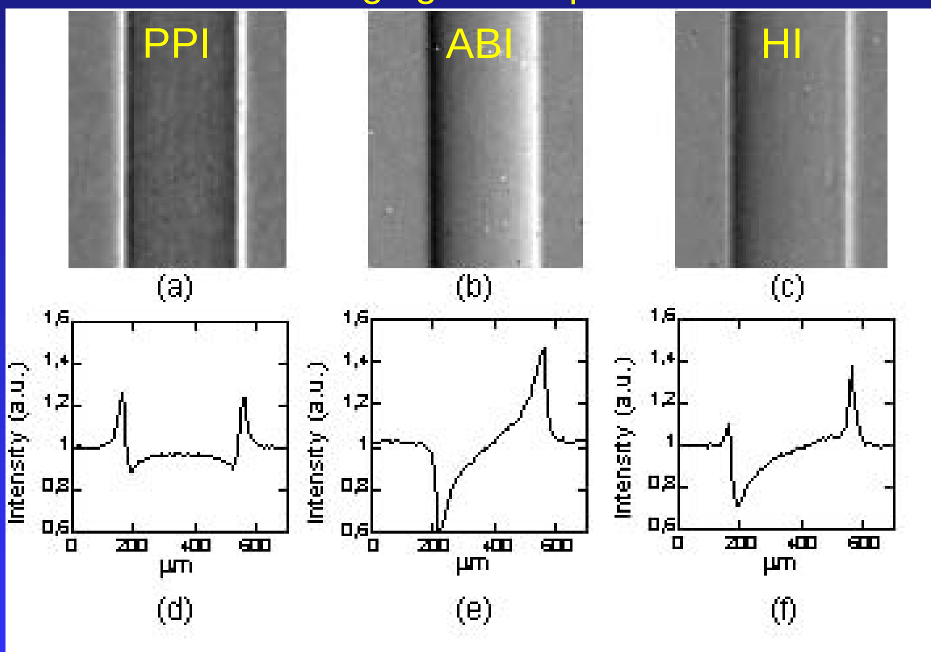

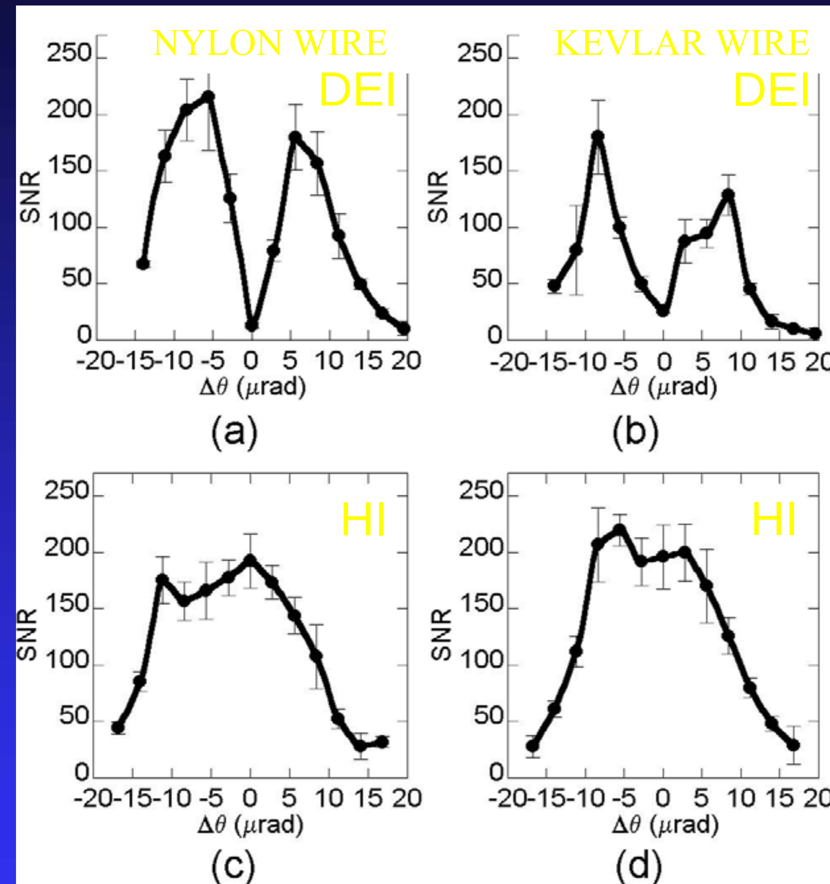

$$SNR = \sqrt{A}\left(I_{\max} - I_{\min}\right)/\sigma_0$$

Signal-to noise ratio values of the signal produced by an edge of the two wires as function of the angular position along the rocking curve of the analyzer for the ABI (nylon wire (a), kevlar wire (b)) and HI (nylon wire (c), kevlar wire (d)) configurations.

P. Coan *et al.*,"Phase-contrast X-ray imaging combining free space propagation and Bragg diffraction," Journal of Synchrotron Radiation **12**, 241-245 (2005)

Radiobiology
Preclinical Radiotherapy
Clinical perspectives

Cancer treatment

- **Surgery**
- **Radiotherapy**
- **Chemotherapy**
- **Gene therapy**
- **+ ….**

• Synergic effects of these therapies are extremely difficult to study and are matter of research for the next (10?20?) years.

• Why a treatment works for a person and not for another is also a central question

Cerebral Tumors

- Epidemiology : 3000 cases/year in France
- 65 % are glioma (high grade tumors)
- Morbidity: short life expectancy (2-36 months)

Cancer of the nervous system is the second most common form of cancer for children, after leukemia

Radiotherapy is only palliative for various tumor grades and locations

- IMRT-Radiotherapy
- 50 Gy at the tumor location
- 25 fractions @ 5/week
- ***Limited by tissue tolerance***

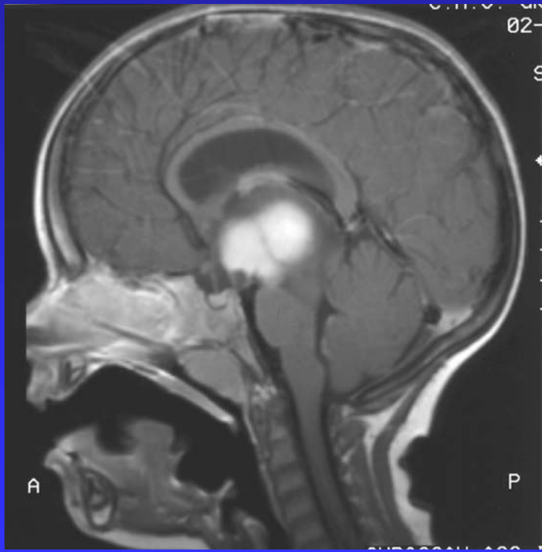

Brain Tumor Radiotherapy: clinical methods

Tomotherapy with 6MV Linac

Gamma Knife

50 Gy at the tumor location
25 fractions @ 5/week
Limited by tissue tolerance

Conventional 6MV source

6 MV Linac-
IMRT, CyberKnife®, X-Knife® etc

BNCT

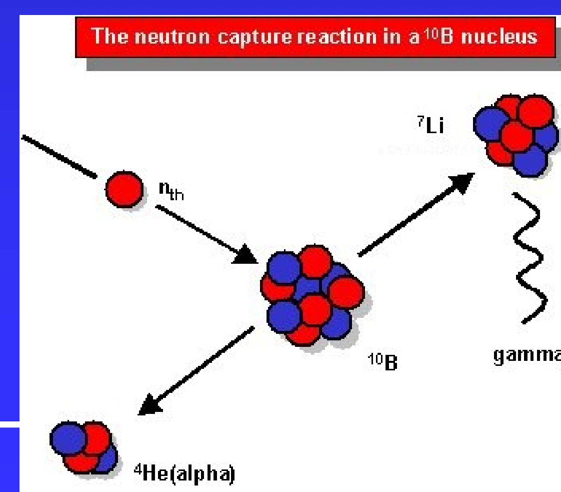

Ultimate Goal of Radiotherapy

- Cessation of tumor growth
- No radiotoxic side-effects

In practice: use of the highest doses tolerated by normal tissues in the vicinity of the tumor

Keywords:

- **Curing effect (reduce tumor size, ablation)**
- **Sparing surrounding tissues**

Optimal dose delivery
(max on tumor, sparing healthy tissues)

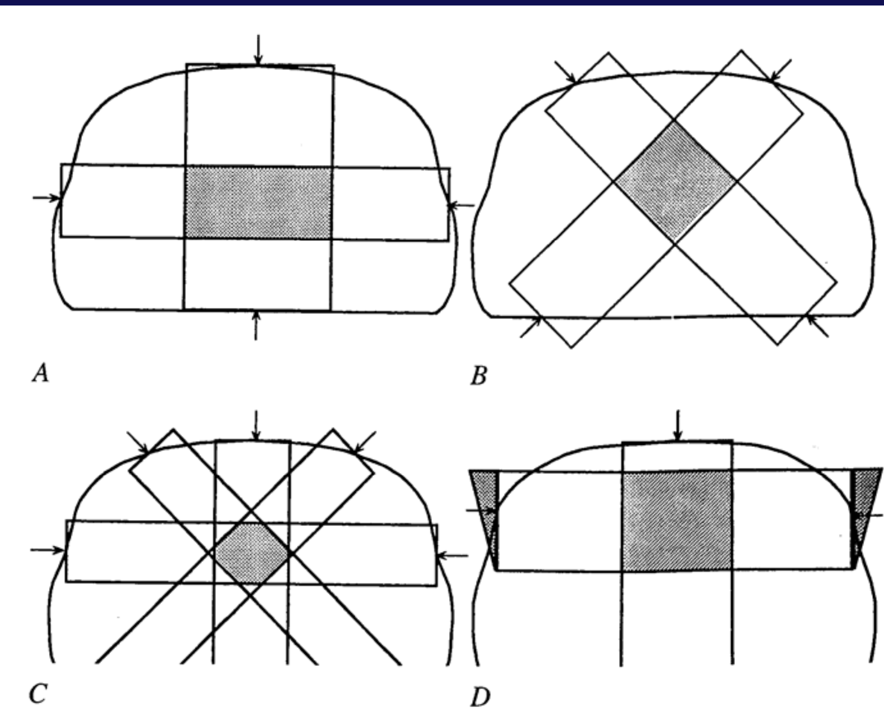

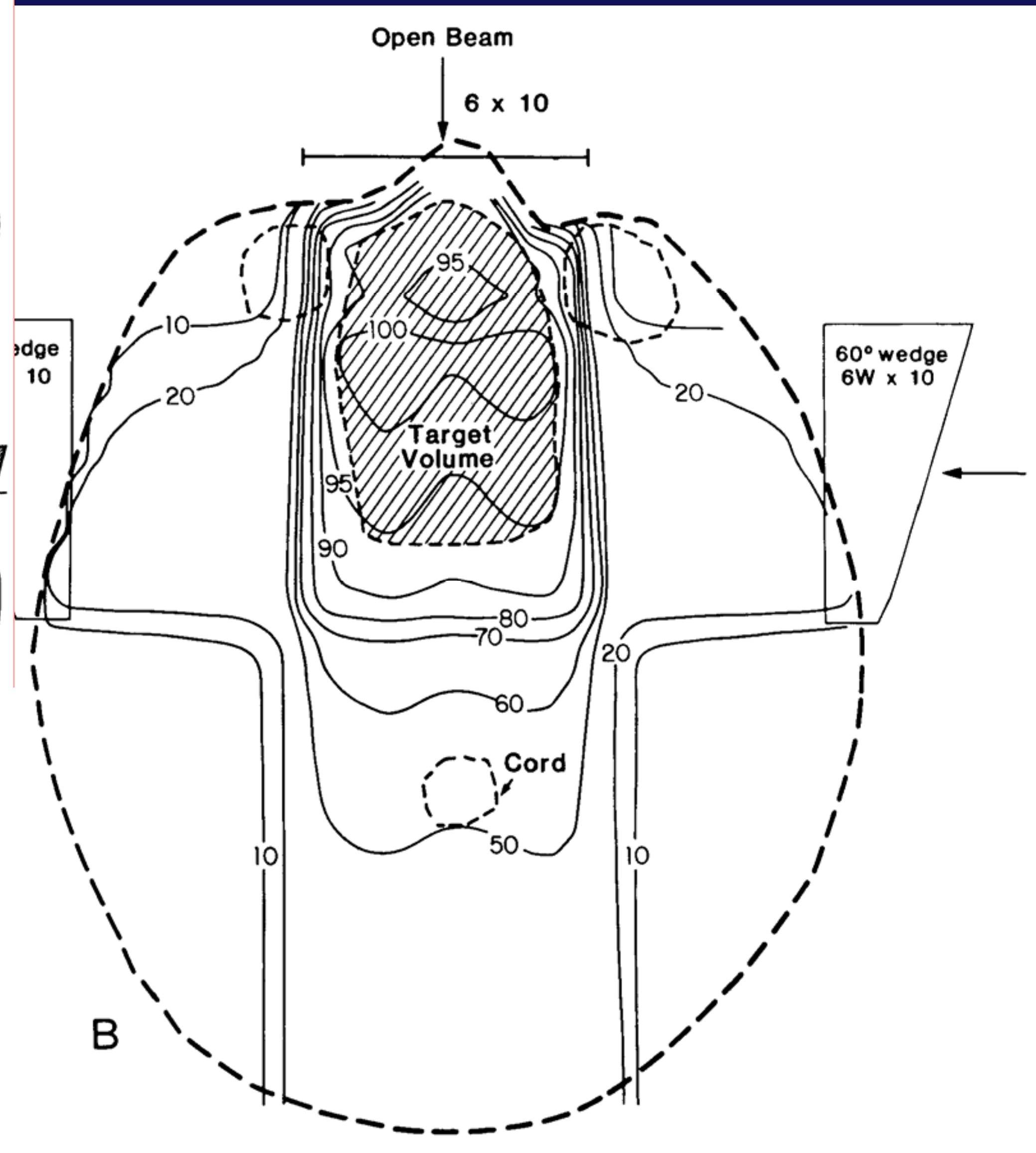

(Traditional?) Biological basis of radiation therapy

1. Cancer cells can be "killed"* by ionizing radiation.

2. Most important target appears to be nuclear DNA.

3. Radiation damage to DNA results in non-viable offspring.

4. Rapidly dividing cell populations are the most sensitive to ionizing radiation (e.g. tumors, epithelial cells, hemopoietic cells (=blood cells formed in the bone)).

………

***"kill a cell"**= cell death, stop multiplication, apoptosis etc.

..but also..

CANCER

One step at a time

David Mooney

Traditional chemotherapy kills tumour cells directly; some newer drugs work instead by cutting the tumour's blood supply. An innovative approach combines these strategies sequentially to pack a double whammy.

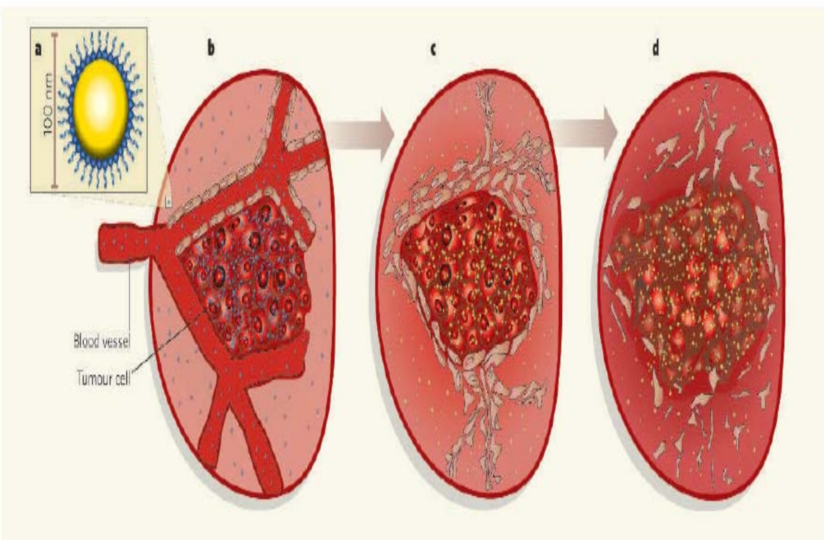

Figure 1 | Step-by-step in fighting cancer. The delivery system of Sengupta *et al.*[2] causes the sequential loss of blood vessels and the death of tumour cells. **a**, Nanometre-scale particles have an outer lipid layer (blue) and an inner core (yellow). **b**, Once injected into the bloodstream, the particle is selectively taken up into tumour tissues, where the lipid layer rapidly releases a drug that kills endothelial cells and disrupts blood vessels. **c**, The inner core gradually releases a chemotherapeutic drug to destroy the cancer cells (**d**).

NATURE | Vol 436 | 28 July 2005

Tumor Response to Radiotherapy Regulated by Endothelial Cell Apoptosis

SCIENCE VOL 300 16 MAY 2003

Radiation-induced bystander effects — implications for cancer

16 | FEBRUARY 2004 | VOLUME 4

NATURE REVIEWS | CANCER

→Tissues, cell reparation, cell communication, protein expression, etc are also key issues in the radiotherapy response

SR is a very good tool to study these mechanisms

Radiation Damage to the DNA

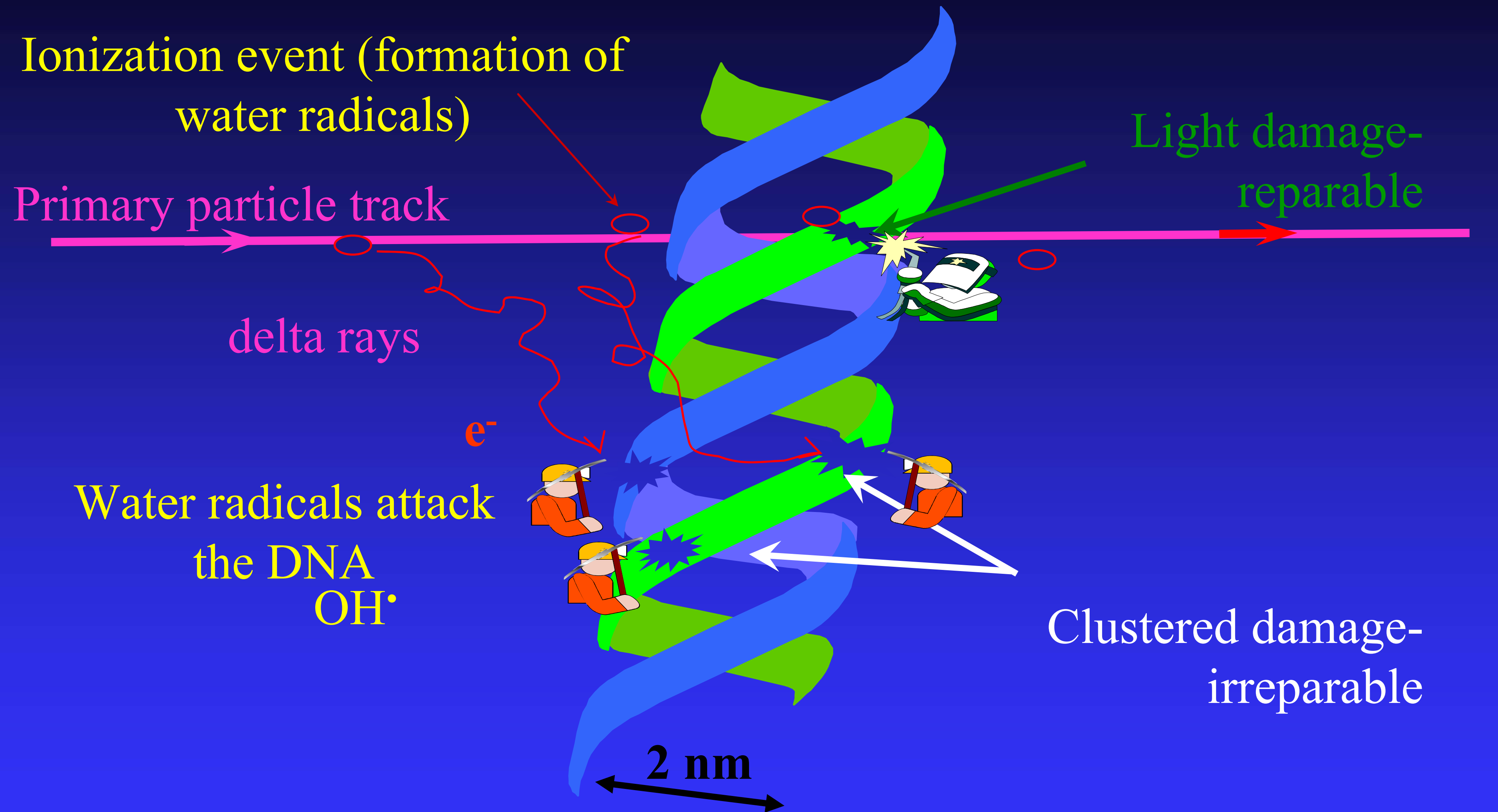

The mean diffusion distance of OH radicals before they react is 2-3 nm

Effect of radiation on cells/DNA

- Cells death is due to not reparable (complex) Double Strand Breaks (DSB) in the DNA
- Cell death: destruction a/o stop of functioning a/o sterility a/o apoptosis
- DSB can be created by 1 or 2 independent events ~40 DSB/cell/Gy, largely repaired
- Bystander effect (Mothersill, *Nature Rev. Cancer 2004*), seems to have a direct link to RT efficiency

Parameters affecting the cell response to radiation

For a given deposited dose and a given cell line, the cell response to radiation depends on:

- dose rate (higher dose rate, higher effect, factor 10 between 0.25 Gy/min and 1.1 Gy/min)
- Temperature
- cell cycle (higher radiosensitivity if in phases M and G2)
- oxygenation (higher radiosensitivity if O_2 reaches environment; free radicals are responsible of 2/3 of DNA damage)

An example: effect of dose rate on mammal cell survival

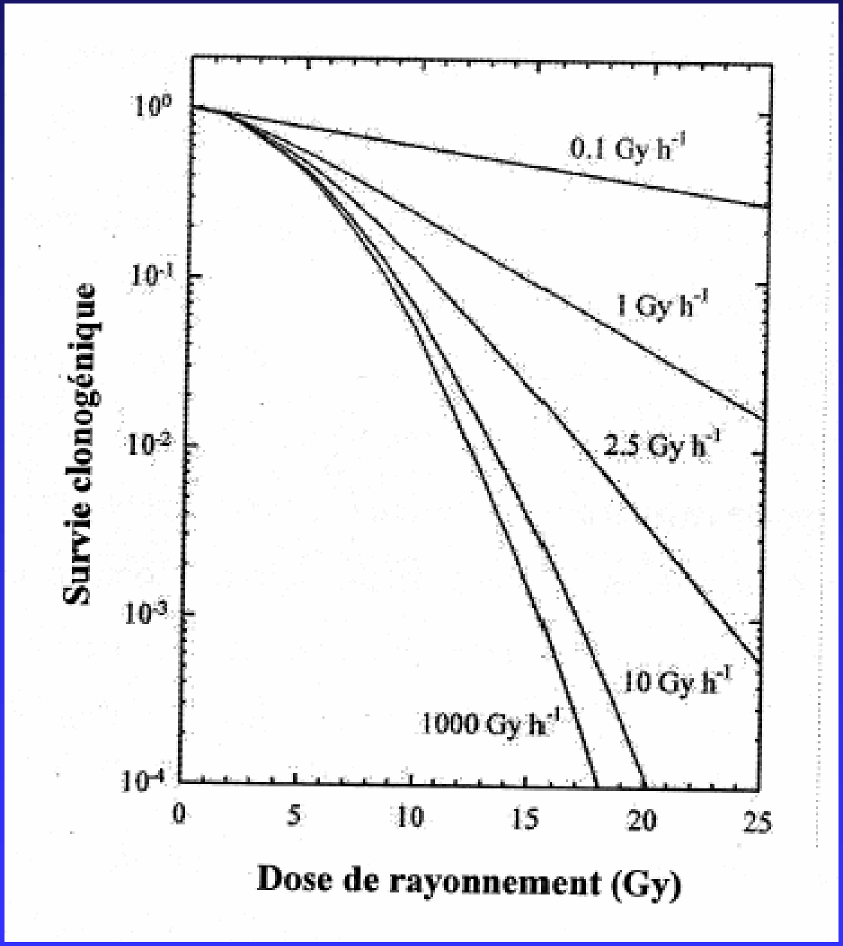

Cell experiments at ID17

1) Incubation, 2) irradiation, 3) development of effects, 4) analysis (counting, molecular biology etc)

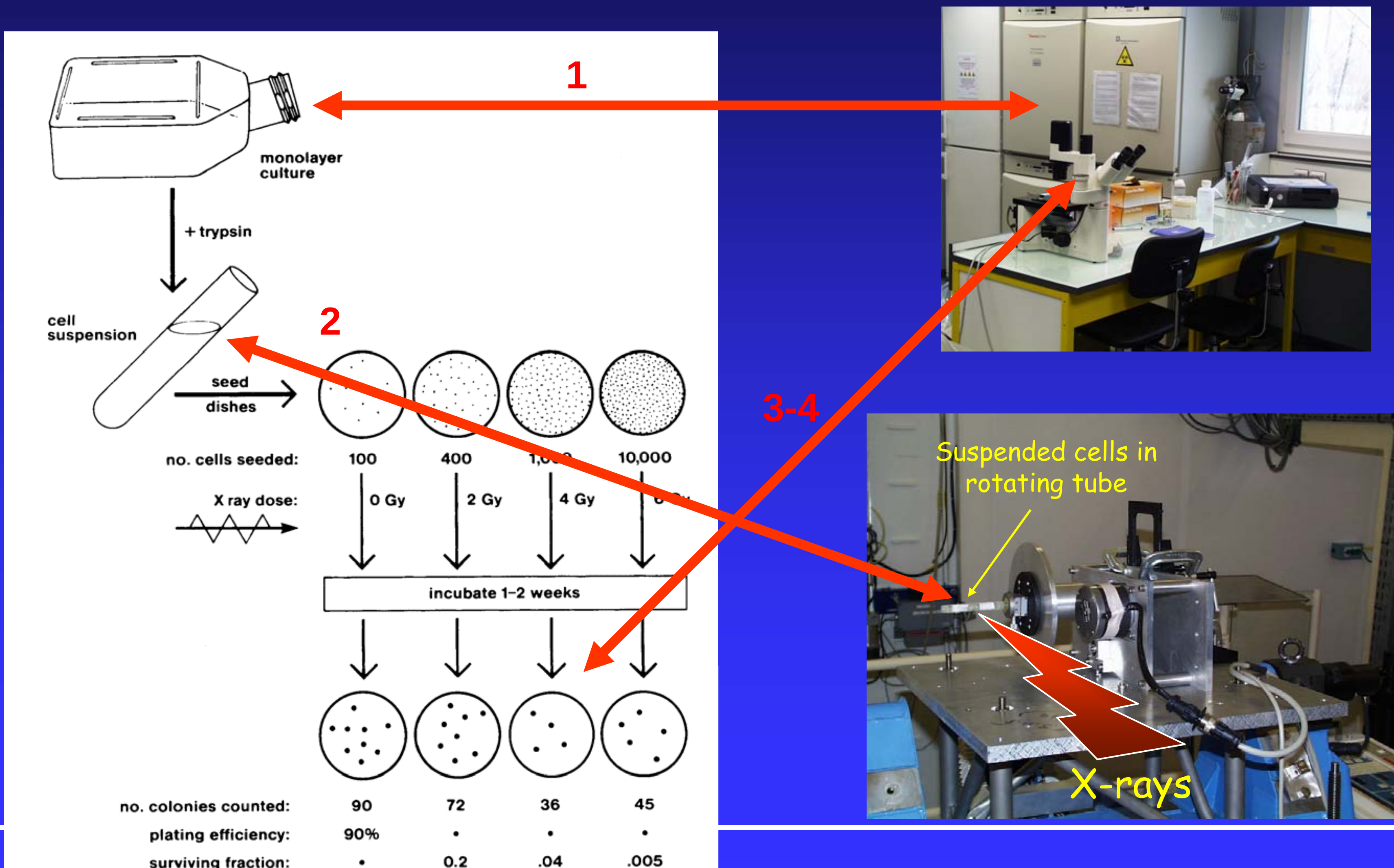

Cerebral Tumors

- Epidemiology : 3000 cases/year in France
- 65 % are glioma (high grade tumors)
- Morbidity: short life expectancy (2-36 months)

Cancer of the nervous system is the second most common form of cancer for children, after leukemia

Radiotherapy is only palliative for various tumor grades and locations

- IMRT-Radiotherapy
- 50 Gy at the tumor location
- 25 fractions @ 5/week
- ***Limited by tissue tolerance***

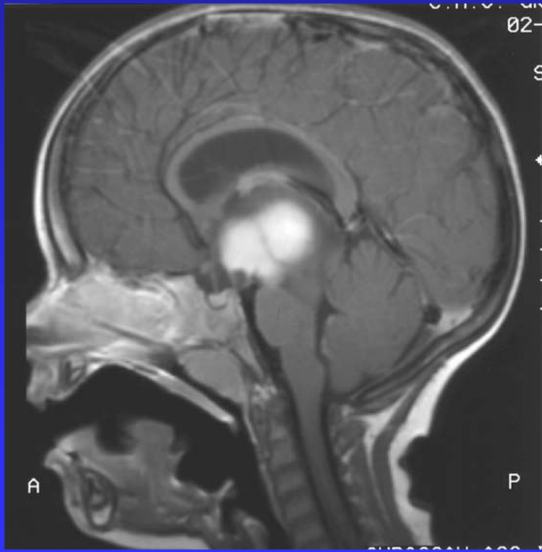

Is there another way for increasing the dose delivered to the tumour while sparing the surrounding tissues ?

Microbeam Radiation Therapy (MRT)

MOUSE BRAIN, VISUAL CORTEX

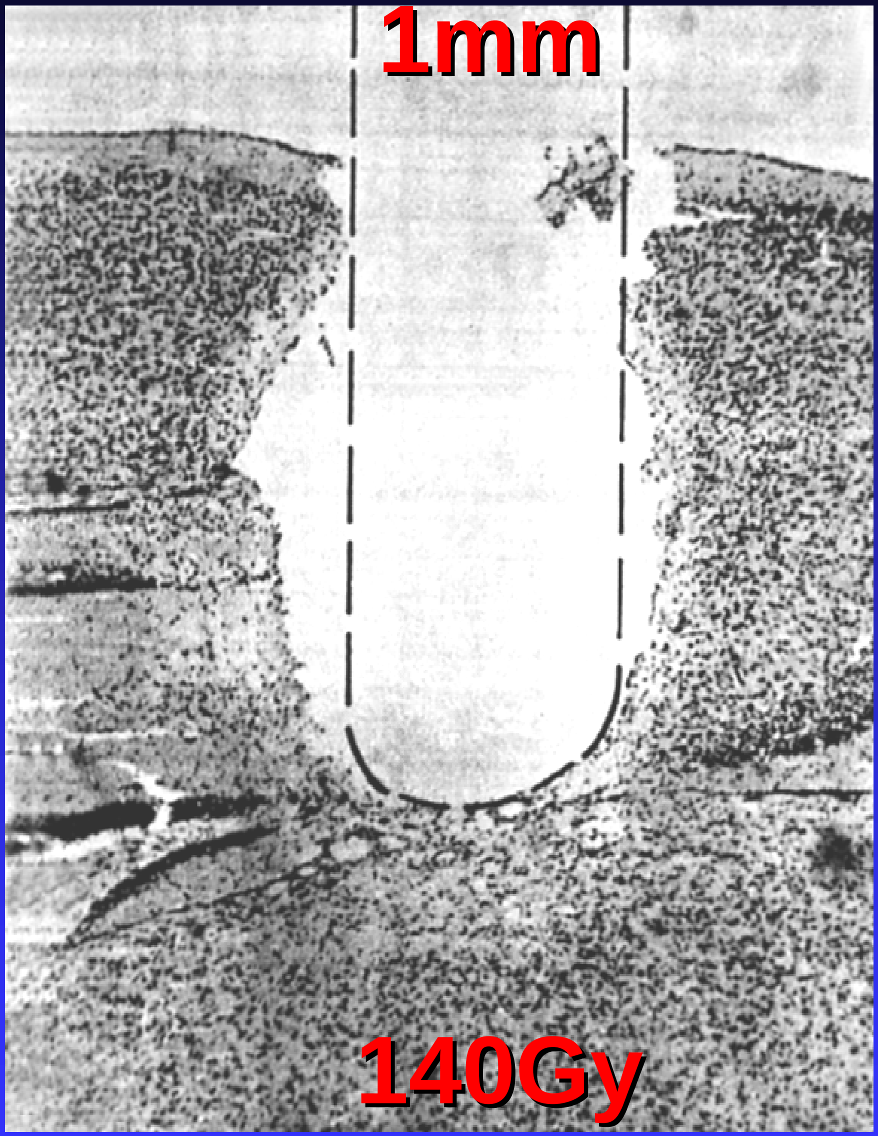

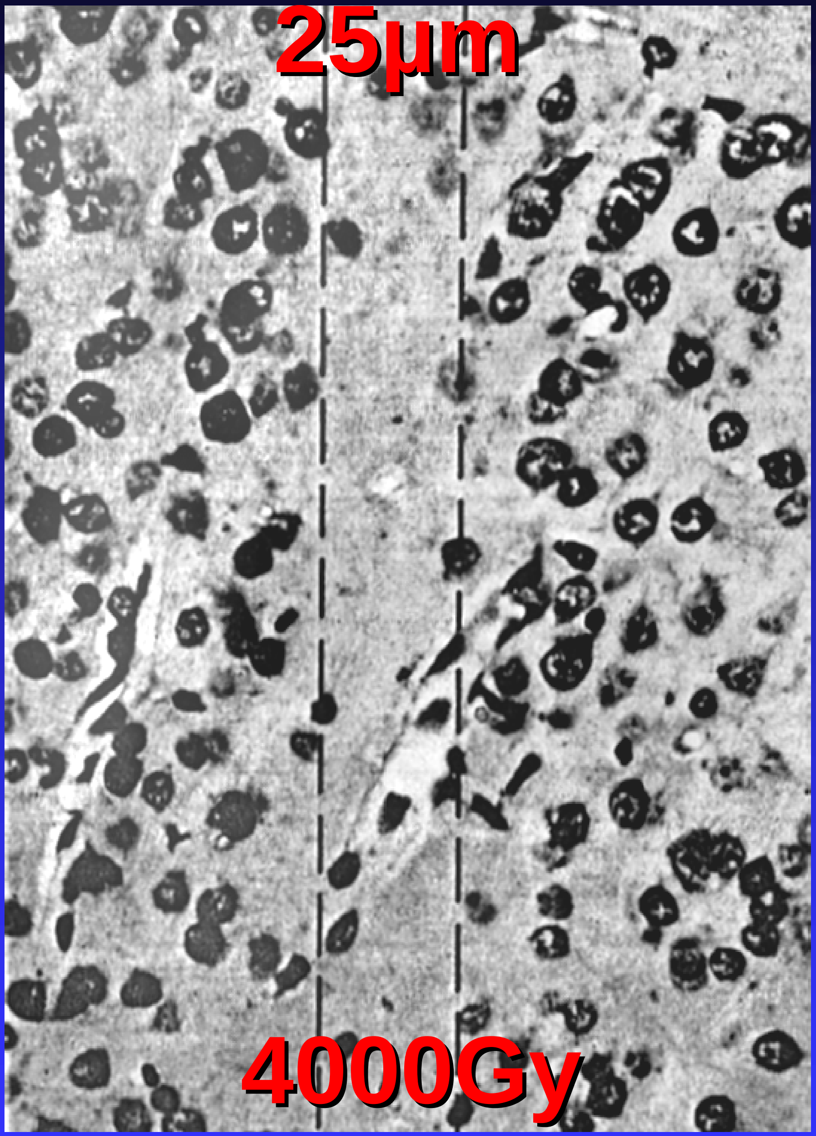

Zeman et al, Radiat Res 15, 496,1961

Dose volume-effect

Beam diameter (μm)		Threshold dose* (Gy)
25	CELLS	4000
75		500
250		360
1000	Tissues	140

*determines the disappearing of cells and/or tissues along the beam path within 24 days after irradiation

Normal brain tolerance to single fraction photons homogeneous, small volume: ≈ 10 Gy *Fike & Gobbel, 1991*

Rat cerebellum after MRT irradiation

Entrance dose: 2000 Gy

25 µm-wide microplane

12 h after irradiation

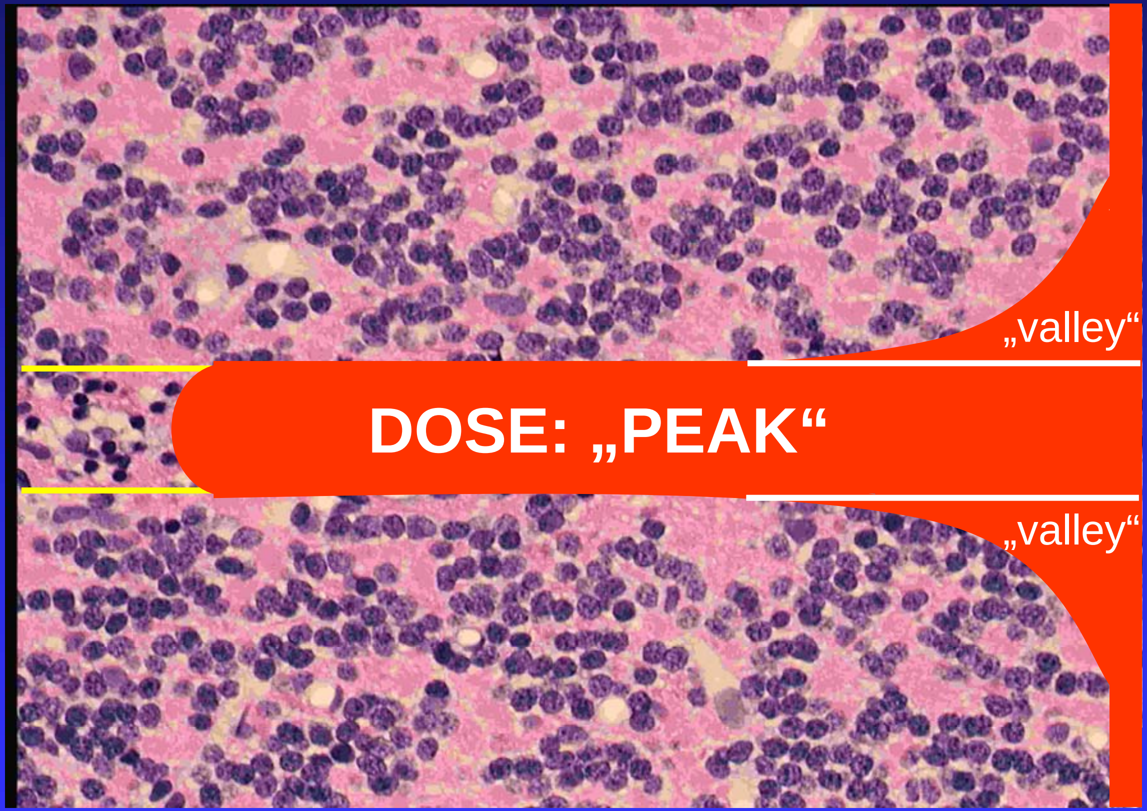

Vascular sensitivity: tumor fragility

Normal **veins and arteries** are composed of three distinct layers of tunics (*interna, media, esterna*). Vessels have a complex and protected structure.

In many kind of capillaries one endothelial cell forms the entire circumference of the capillary wall

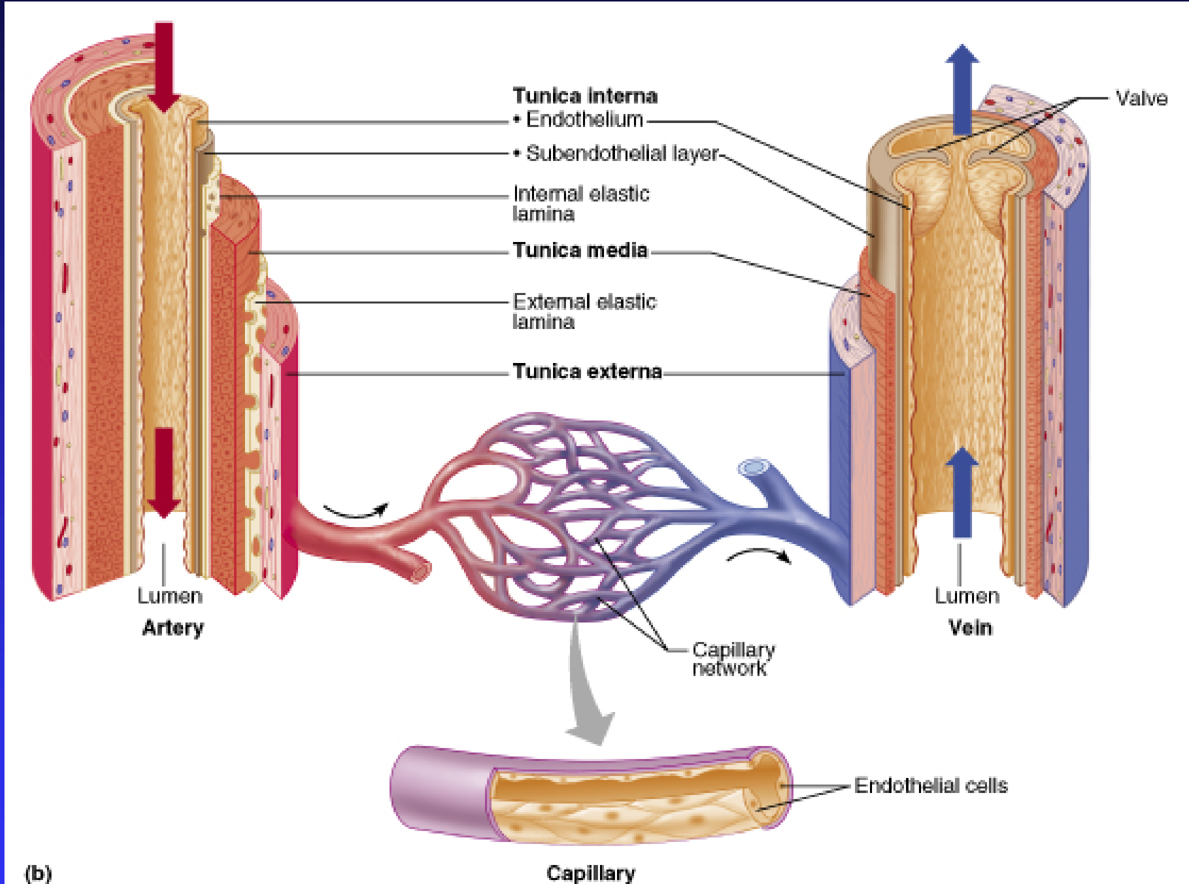

Tumor vasculature has only one endothelial cell layer
And is more fragile!!!

Pictorial microbeam-vasculature interaction

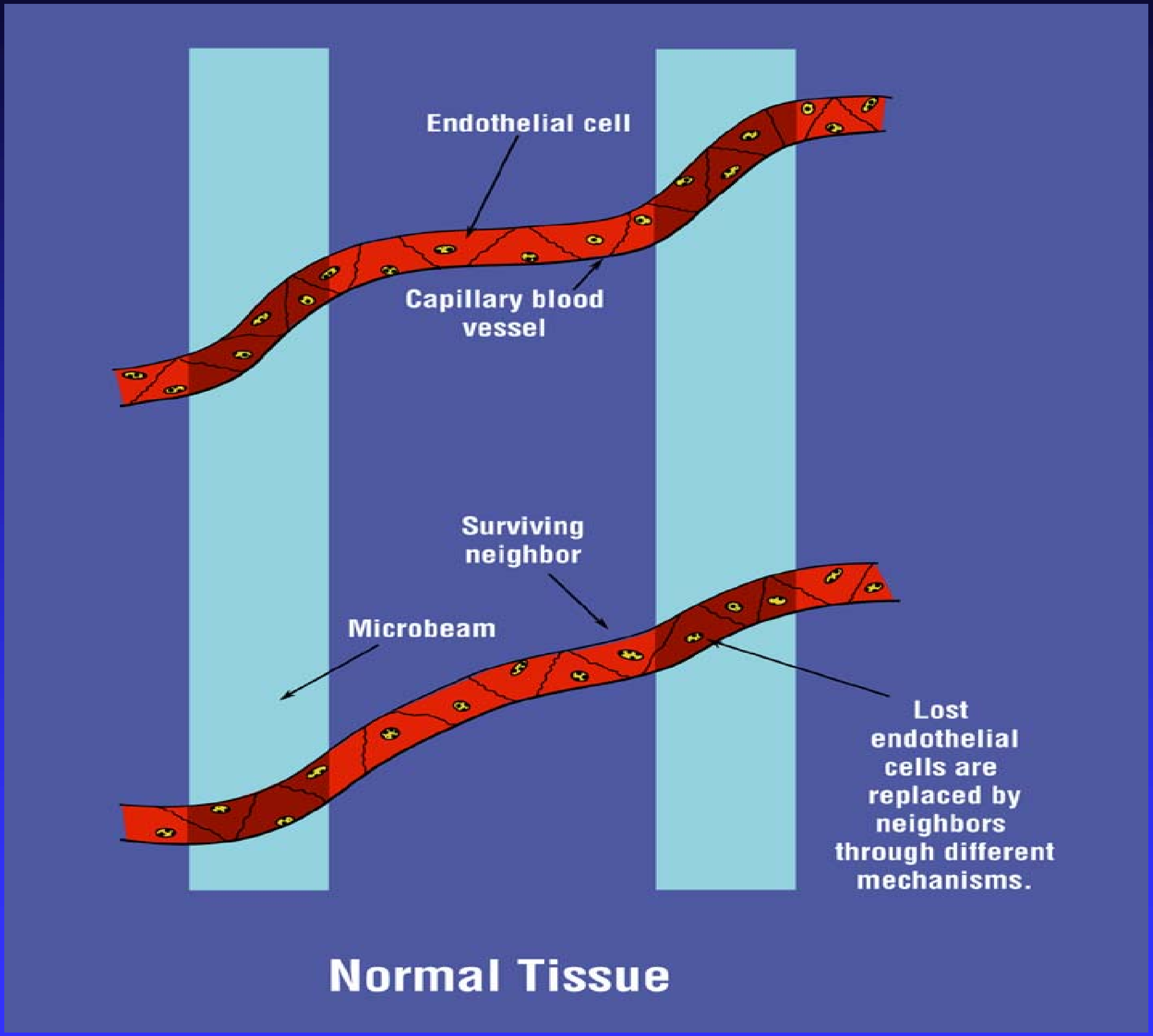

MRT beam requirements: ESRF ID17 source

High intense, collimated, hard X-ray beam (~100 keV)

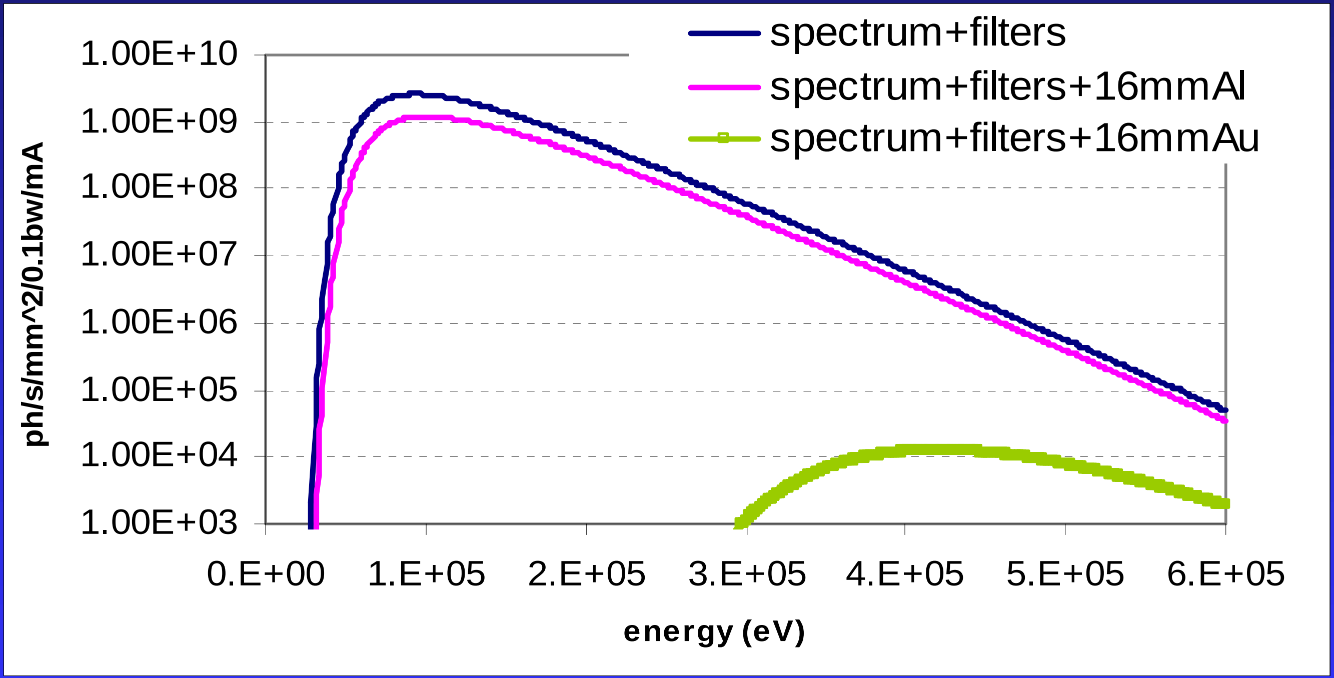

- Wiggler: 21 poles, 1.6 T
- Filters: 2.4 mm Al, 1.4 mm Cu
- Dose rate: 14300 Gy/s @ 200 mA from source

Microbeam production

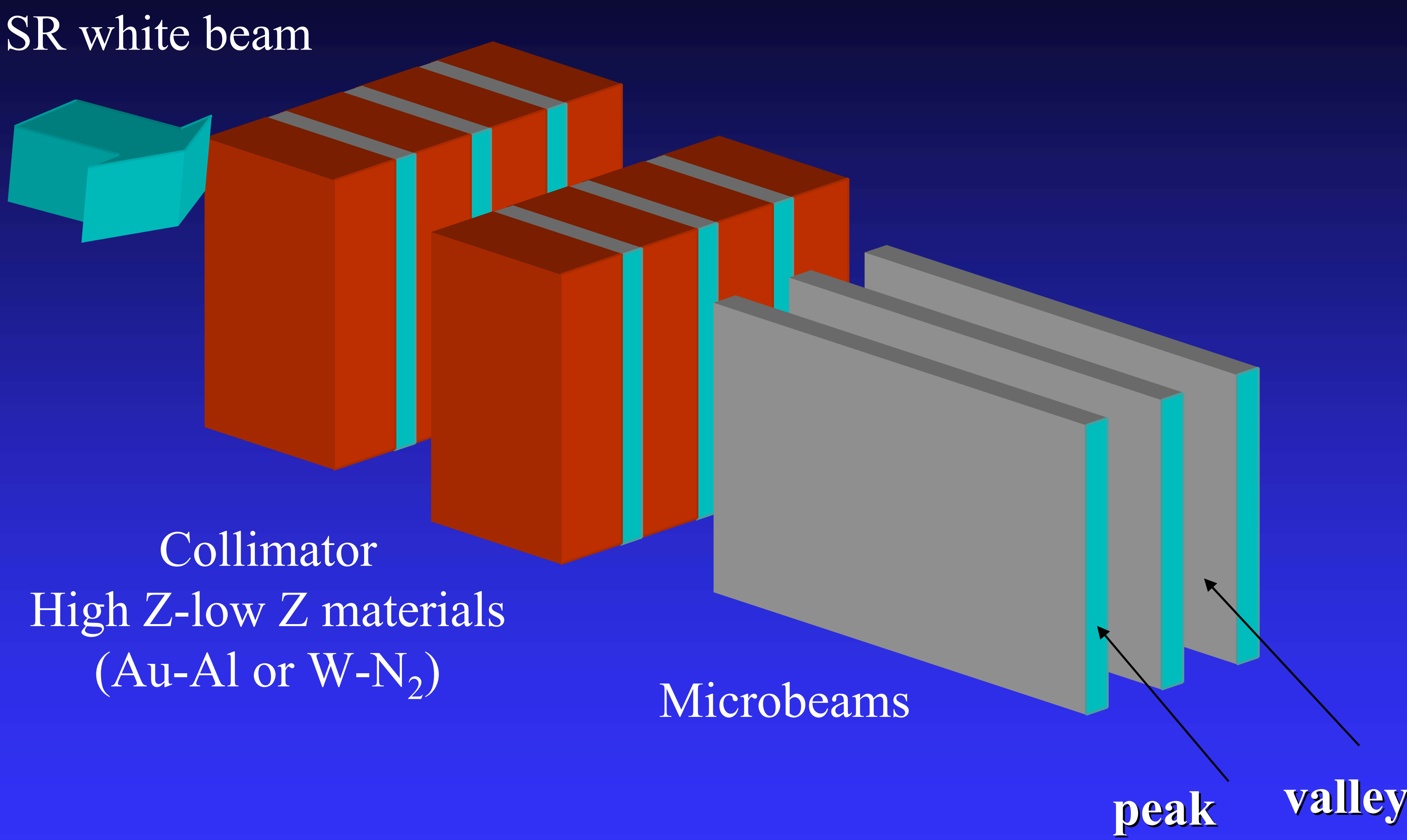

Microbeam: variable width (0-100 μm), 100-400 μm pitch

50-125 microbeam array to cover up to 5x5 cm^2

Why SR to MRT?

- Extremely high dose rate is needed to irradiate the tissues in a fraction of a second (avoid smear out of beams due to hearth beat)
- (Quasi) Parallel beam for fractionate the X-ray beam
- Optimal energy for maximum PVDRs (~150 keV)

Conventional sources are not adapted

The importance of Peak to Valley Dose Ratios (PVDRs)

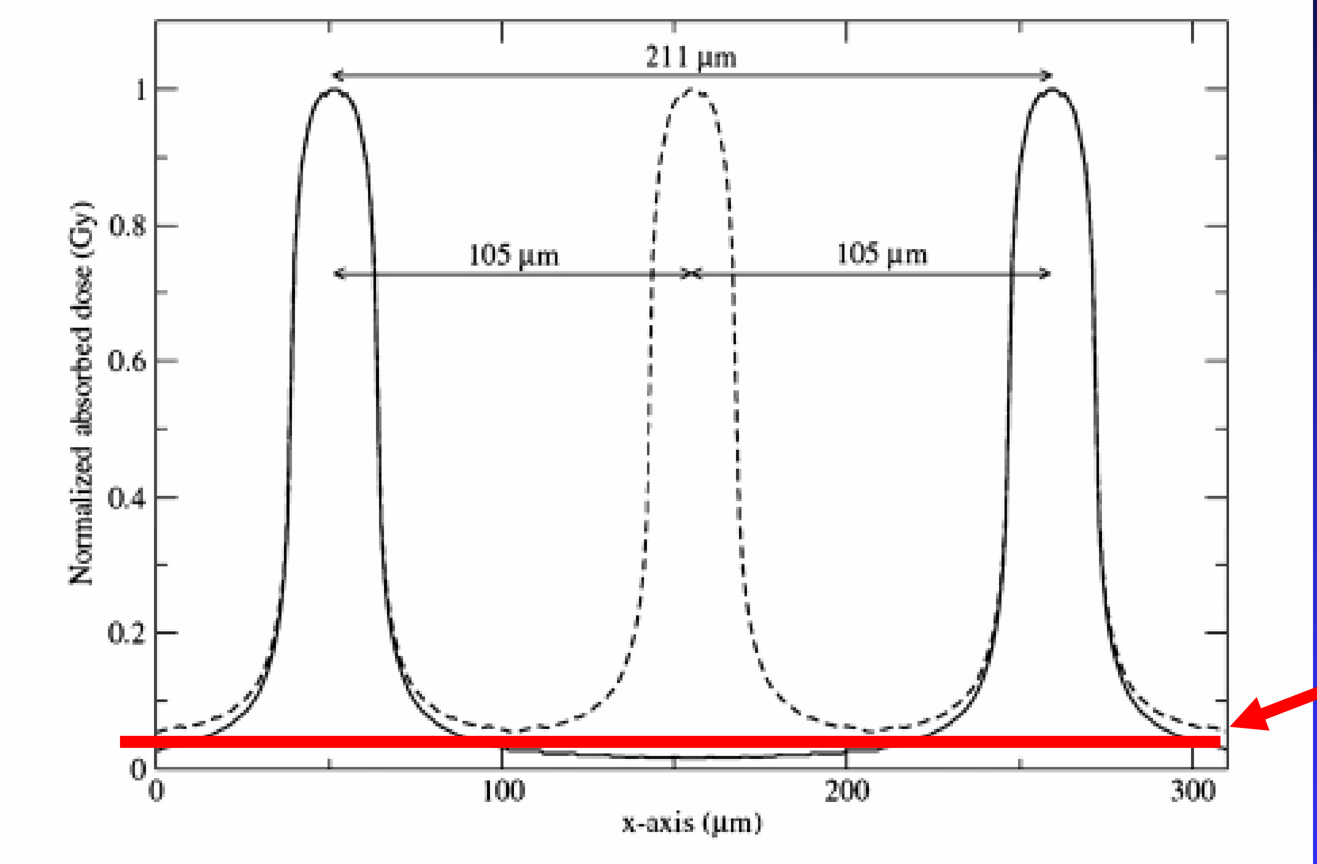

Tissue tolerance threshold dose for healthy tissue homogeneous irradiation

The dose in the valleys that creates a dose offset in the tissues, has to be below the tolerance threshold dose

The PVDRs dependencies

- X-ray energy spectrum
- Sample size and composition
- Microbeam width and c-t-c distance
- Irradiation field and depth

Photons in water

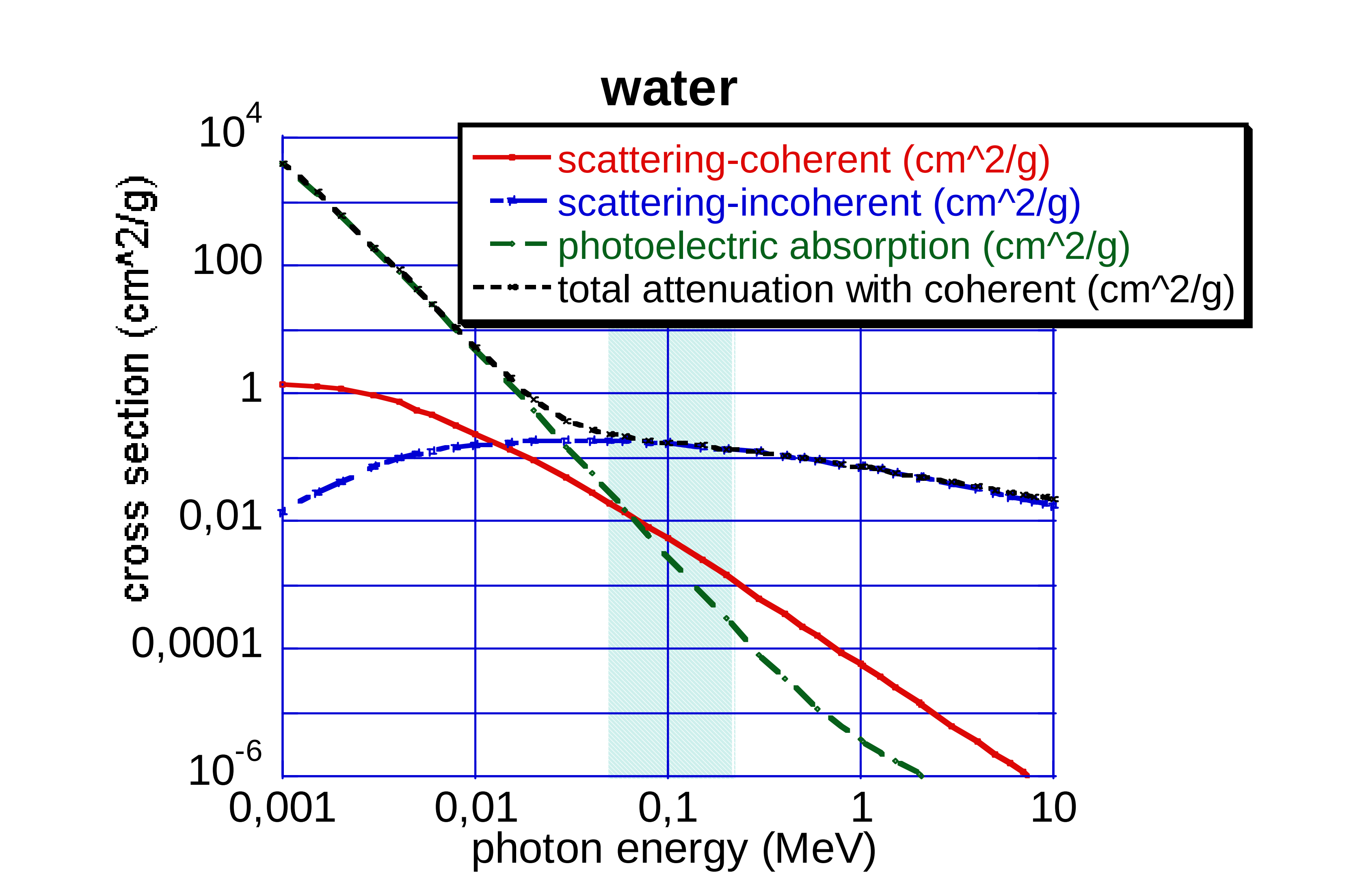

Compton scattering is predominant in the energy range of interest (consequences on dose and angular distribution).

Electrons in water

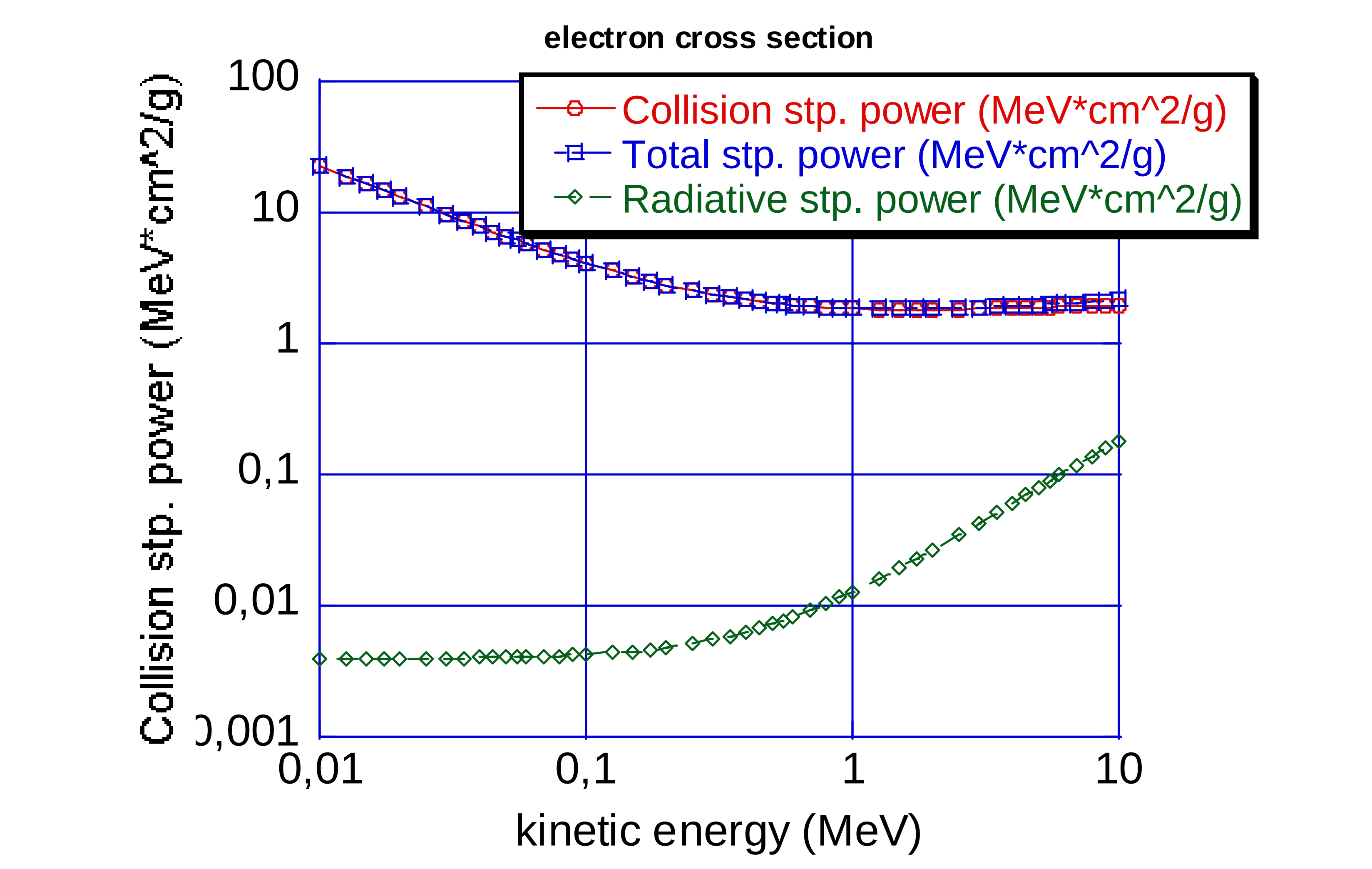

Ionization is the most important process, which leads to large part of energy deposition

(Simplified) set-up for MRT

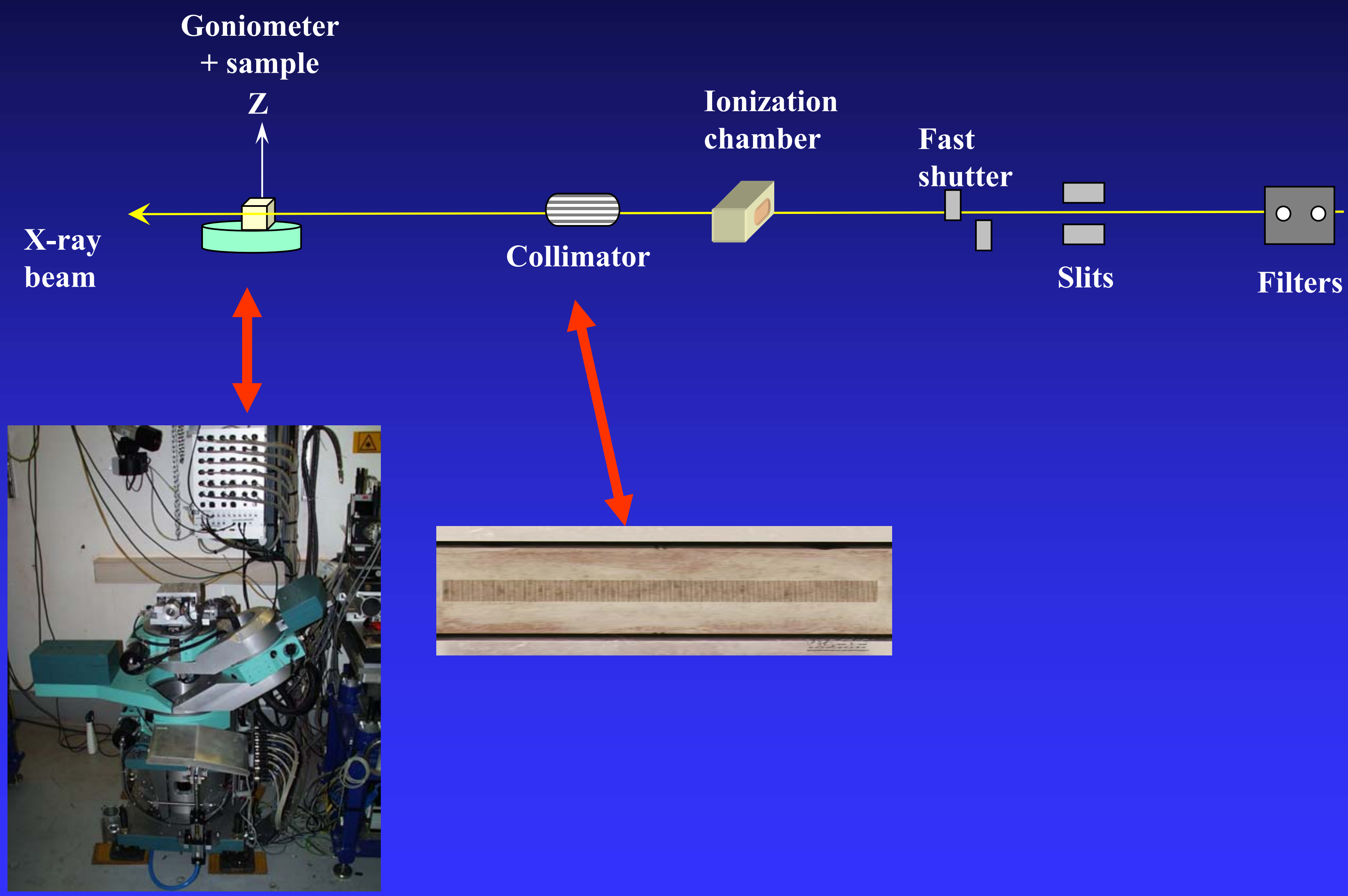

E. Brauer-Krisch, et al. Rev. of Scientific Instr. 76, 064303 1-7 (2005)

Curing effect of MRT

MRT+ Gene-therapy targeting brain tumours (gliosarcoma) in rats

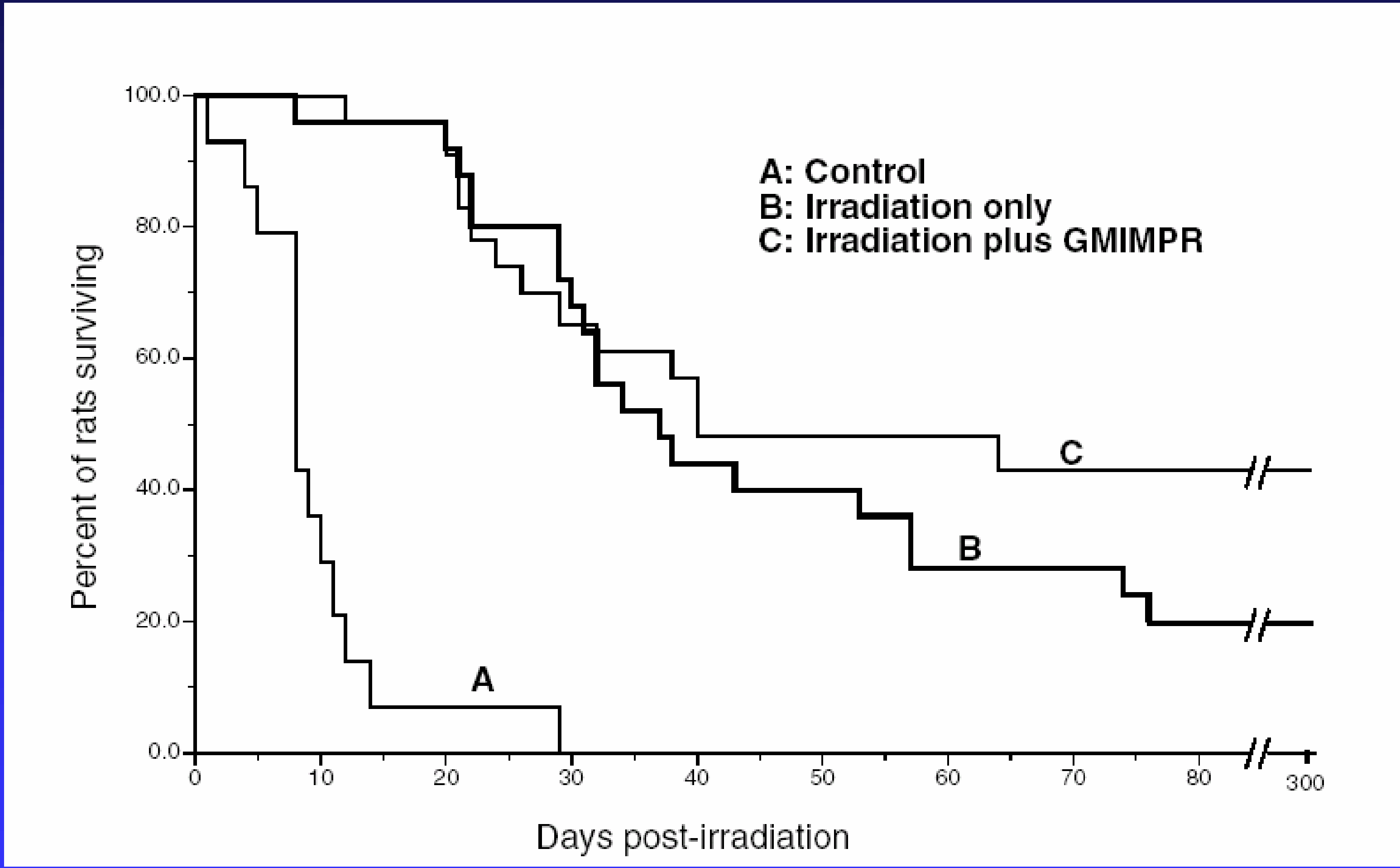

H. Smilowitz et al. J. Neurooncology, 78: 135–143 (2006)

Stereotactic Synchrotron Radiation Therapy (SSRT)

SSRT

- Principle:
  - Tumor loaded with a high Z element (iodine, gadolinium) + a chemotherapic drug (cis-platinum)
  - Beam size adjusted to the tumor dimensions
  - Tumor positioned at the center of rotation
  - Irradiation with kilo-Voltage X-ray beam

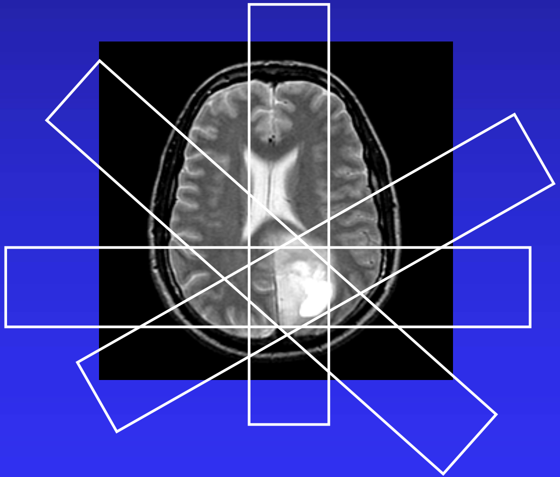

Why SR to SSRT?

- Energy Tuning
  - ⇨ Obtain a maximum dose enhancement effect
    Bone X ray dose reduced

- Monochromatic beam
  - ⇨ Avoid beam hardening effect
    Improve dose uniformity in the tumor

Quantitative Computed Tomography
  - ⇨ Absolute contrast agent concentrations
    Precise dose estimation

Iodine Dose Enhancement

- Tumor > Blood Brain Barrier disruption
- Accumulation of the contrast agent
- Tumor X-ray absorption cross section is increased ($Z_{iode} >> Z_{eq.water}$)

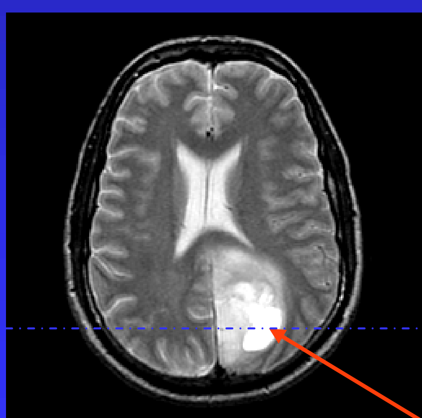

Tumor

Dose Profile

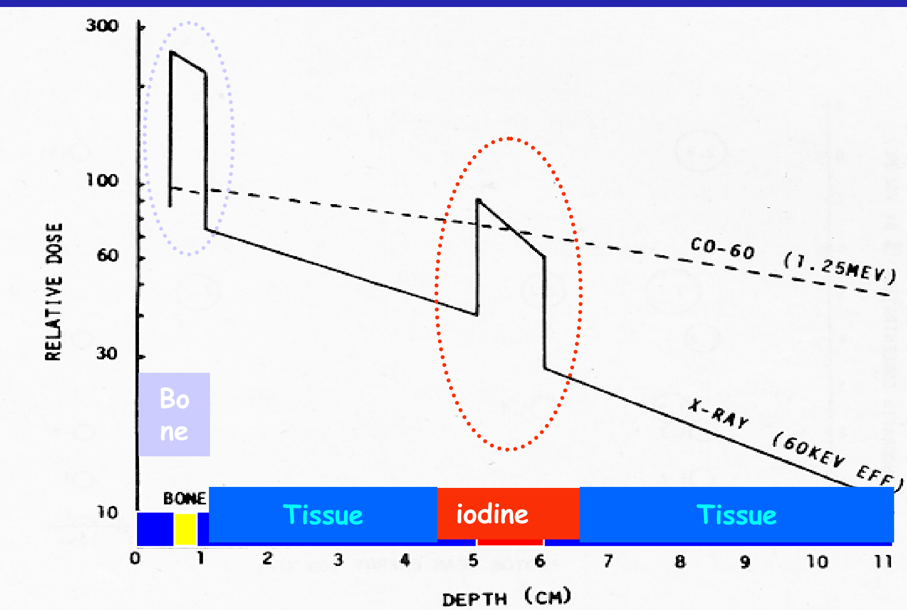

FIG. 2. Depth dose distribution (calculated).

Survival vs Iodine Concentration

- ✓ Just after irradiation ⇒ Cells were sub-cultured
- ✓ 15 days later ⇒ Colonies were stained and counted

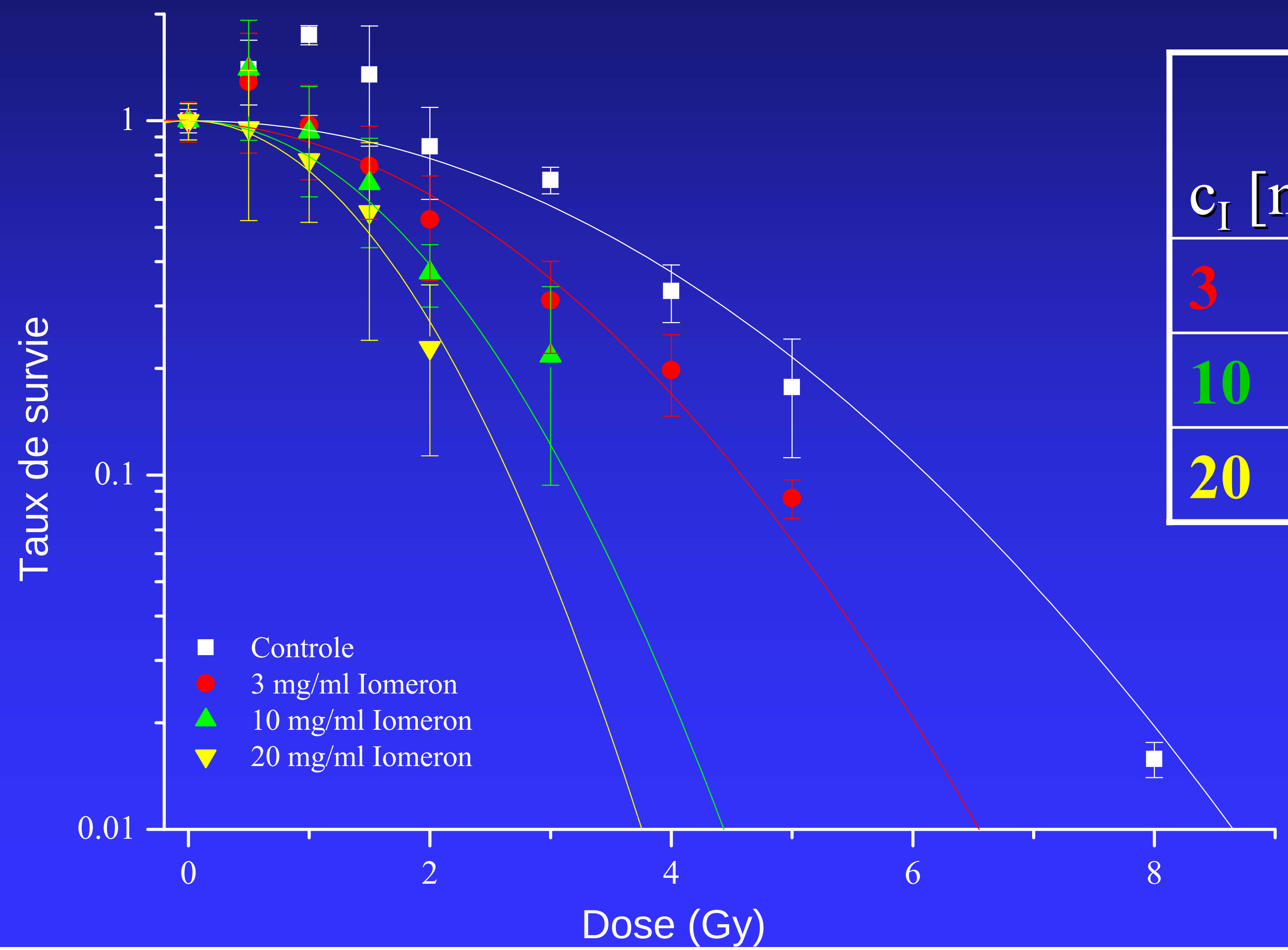

c_I [mg/ml]
3
10
20

Energy: 50 keV

Preclinical studies

- Tumor model: F98 glioma
- Animal model: (Fisher) Rat

iodine…..

Tumor is irradiated (15 Gy) after infusion of iodine (2 ml, 350 mg/ml)

Enhancement life span: +170 %

JF Adam et al. Int J Radiat Oncol Biol Phys. 2005 61 (4) 1173-82
JF Adam et al. Int J Radiat Oncol Biol Phys. 2006 64 (2) 603–611

Dose distribution vs iodine concentration in the target

(calculated via Monte Carlo, MCNP code)

Energy: 85keV

- Beam height : 2 cm
- Beam width : 2 cm
- Iodine: 10 mg/ml

Isodose lines:

red = 90%,

green = 50%,

blue=25%

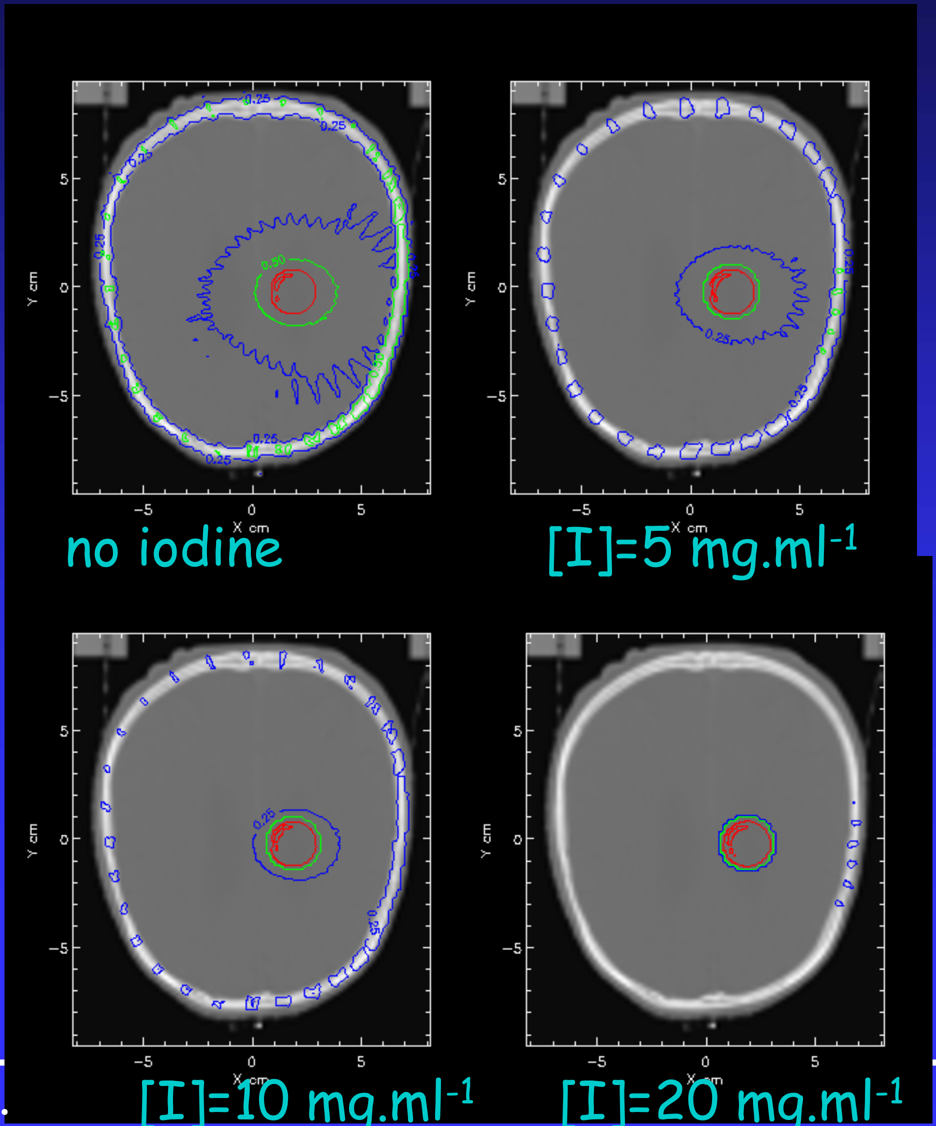

C. Boudou et al. Phys Med Biol. 2005 Oct 21;50(20):4841-51.

Inoculation of a Platinum compound (PAT)

- (CDDP)-Platinum compound
- Chemotherapy agent
- CDDP binds to DNA
- Intra-tumor injection of 3 mg CDDP in 5 ml, 13 days after tumour implantation
- Irradiation @78 keV - 15 Gy @ tumor - Day 14th

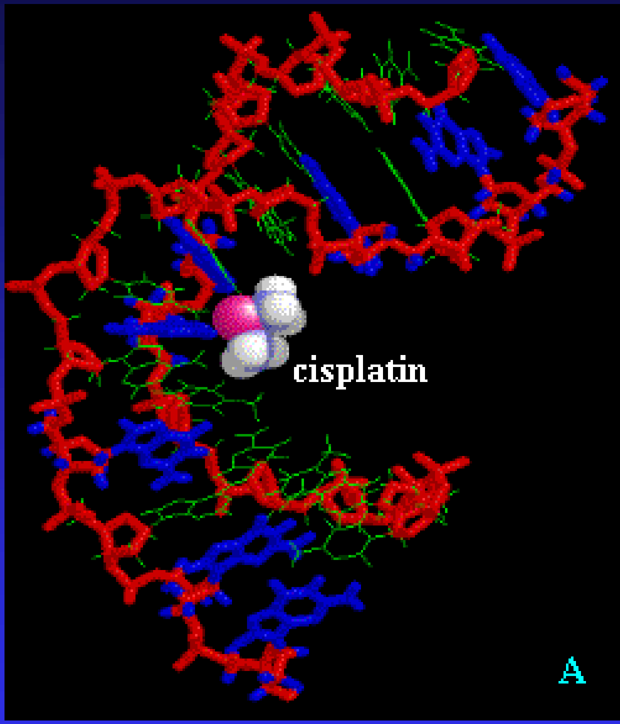

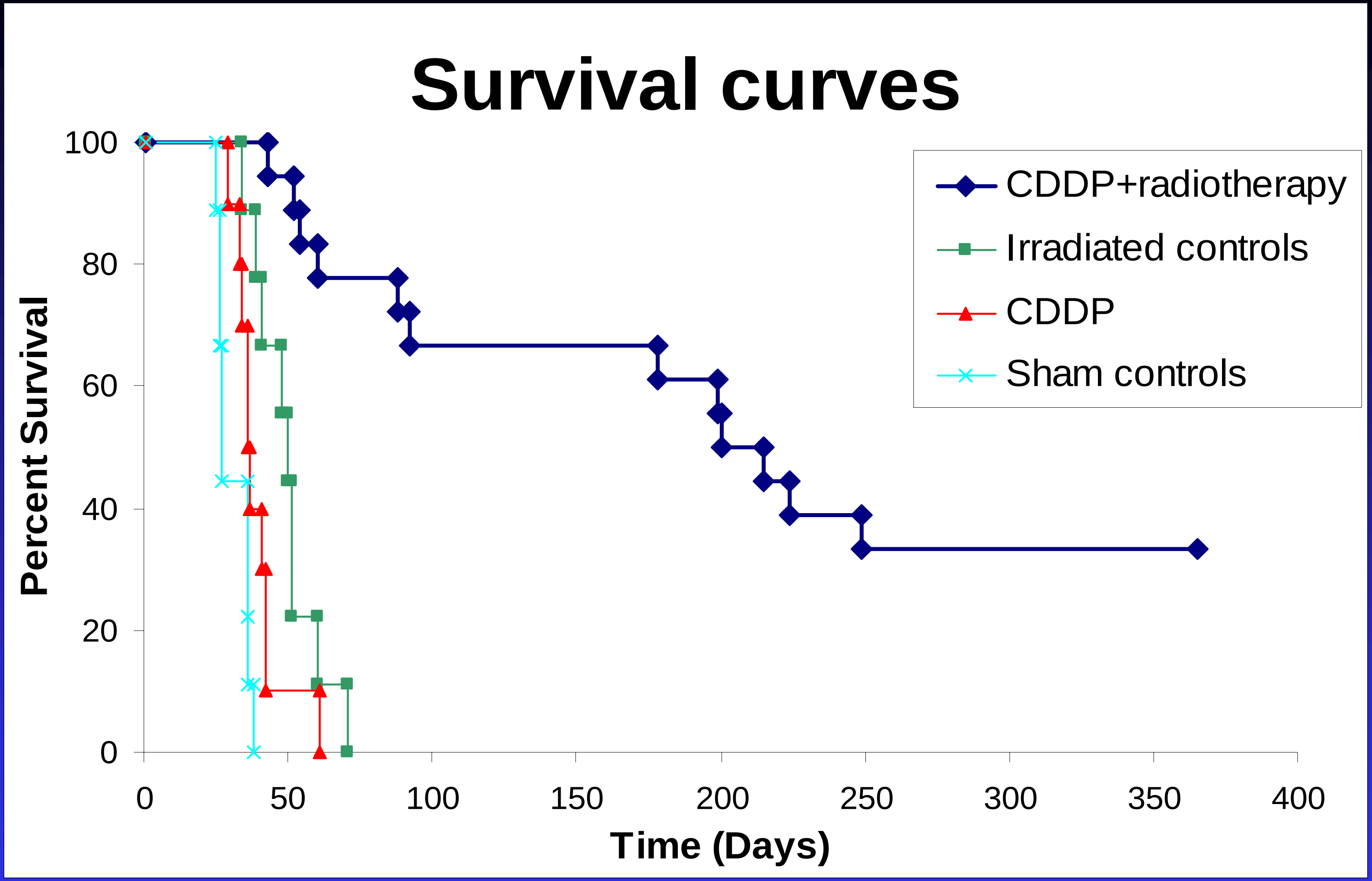

694 % Increase in life span relative to median survival time

M.C. Biston, et al., Cancer research, 64, 2317-2323 (2004)

Clinical perspective of MRT and SSRT at the ESRF

- Following excellent preclinical results, the ESRF and CHU Grenoble have decided to perform SSRT clinical trials at ID17. The protocols and technical refurbishment are under preparation.

- The ESRF has also decided to fully refurbish the MRT station for allowing testing the therapy in spontaneous tumours in animals.

Thank you all for the attention!!

Acknowledge for slides:
ESRF-INSERM team
ID17 team